RESPONSE TO COMMENTS BY HARZA-EBASCO SUSITNA JOINT VENTURE ON AEIDC'S REPORT ENTITLED "STREAM FLOW AND TEMPERATURE MODELING IN THE SUSITNA BASIN, ALASKA."

Response to Comments by Harza-Ebasco Susitna Joint Venture on AEIDC's Report Entitled "Stream Flow and Temperature Modeling in the Susitna Basin, Alaska"

Alaska Resources Library and Information Services (ARLIS) is providing this table of contents.

Table of Contents

SUS #218

Part 1:

Harza-Ebasco Susitna Joint Venture

Comments on AEIDC report

"Stream Flow and Temperature Modeling in the Susitna Basin, Alaska.

HARZA-EBASCO SUSITNA JOINT VENTURE

Design Office: 400-112th Avenue, NE Bellevue, Washington 98004 Tel. (206) 451-4500
Main Office: 8740 Hartzell Road Anchorage, Alaska 99507 Tel. (907) 349-8581

August 9, 1983
4.3.1.4

AUG 11 83

Dr. William Wilson
Arctic Environmental Information & Data Center
707 A Street
Anchorage, Alaska 99501

Subject: Susitna Hydroelectric Project
Report on Stream Flow and Temperature
Modeling in the Susitna Basin, Alaska.

Dear Bill:

Attached are our comments on the AEIDC report entitled "Stream Flow and Temperature Modeling in the Susitna Basin, Alaska." In general, we felt that the report is well written and provides a good documentation of the modeling effort of AEIDC.

We have several specific comments to which we would like your responses. If it is efficient, please revise the draft report where appropriate in response to these comments. However, many of the comments may be more appropriately addressed in a separate memorandum.

When the report is final, please submit twenty five copies which we will distribute to the appropriate entities.

Sincerely,

John R. Bizer, Ph.D.
Lead Aquatic Ecologist

JRB:baj

cc: G. Lawley, H-E
E. Marchigiani, APA
attachments

COMMENTS ON AEIDC STREAM FLOW AND TEMPERATURE MODEL

General Comments:

Generally we found the AEIDC stream flow and temperature model to be a well written document. It provides a thorough and theoretical approach to the determination of stream temperatures. However, since the report was written for a technical audience, we would have preferred a more detailed description of the various submodels rather than a reference to Theurer et al. 1983.

We question whether AEIDC's use of three methods to determine subbasin flow contributions was worth the expenditure. While we do not object to assessing the relative differences amongst methods, we wonder why the computations were made for all subbasins for each method. The time variation of these contributions may be important and has not been considered.

We also question whether the technique to determine the distributed flow temperatures is more sophisticated than is necessary. We would recommend using available historical tributary temperature data and perhaps correlating this with air temperatures to generate a tributary temperature time series. We doubt that errors in estimating tributary temperatures will have a significant effect on mainstem temperatures.

We would like to see a daily prediction of mainstem temperatures, as we feel monthly temperatures may be too coarse to properly assess project impacts. This will not only be necessary for the instream ice study but has also been requested by the resource agencies. We will need to examine the effect of high, medium and low flows on stream temperatures. Water years 1981, 1982 and 1974 have tentatively been selected for this purpose. We would like to see sensitivity tests using various meteorological sequences with each of the flow conditions.

We do compliment AEIDC for incorporating a shading factor and accounting for tributary inflow in the model. These are two significant improvements over the HEATSIM model.

SPECIFIC COMMENTS

p.1 Par. 2	Note that ADF&G and USFWS have undertaken studies of temperature effects on salmonid egg incubation.
p.8 Par.1 & p.11 Par. 2	Since subjectiveness is involved in areal precipitation weighting (method 2), is using this method more appropriately than using the drainage area method? Since Method (2) yields a higher Watana discharge, we recommend this method not be used at this time. The high discharge implies additional economic benefits. For economic runs, we need to be conservative. However, a final decision on the selected method will be made by H/E in the near future.
p.9 Fig. 3	Mean annual water yield for several subbasins appears to be greater than the mean annual precipitation (Tsusena, Fog, Devil, Chin-Chee, Portage).
p.10,Bottom	Calculated C_w for Method (1) is 0.5104. Acres used 0.515. Why is there a difference? Were areas replanimetered?
p. 18, Par. 1	We suggest using solar radiation measurements when available rather than calculated values. We would also like to see daily comparisons of observed versus computed solar radiation. Please provide descriptions of the six SNTEMP submodels.
p.19,Bottom	More discussion on heat flux would be helpful. Statements regarding the relative importance of heat inputs and outputs should be made. Please provide all heat sources and sinks considered.
p.20	In Eq. (9), how was T_e(Equilibrium temperature) estimated? What are the parameter values of K_1 and K_2?
p.21	There are potential problems with using temperature lapse rates at Fairbanks and Anchorage. Both sites are subject to temperature inversions because of topography. This may not occur along the Susitna River. We recommend that the existing Weather Wizard data be reviewed.
p.24,Par 4	How have we demonstrated that topographic shading has an important influence on the Susitna River? While we do not dispute this, we would like to see this verified with a sensitivity run.

p.27,Par.2 — Stream surface area is necessary to compute heat flux. According to Figure 26, we are considering only ten (10) reaches. How representative are these reaches for determining stream width and hence surface areas for the river segment between Watana and Sunshine? While Appendix B illustrates the representativeness of the ten (10) reaches,it appears that we may have lost some of the refinement of the Acres model with its approximately sixty (60) reaches.

p.29, Par.1 — To compute daily minimum and maximum temperatures, we suggest the use of HEC-2 velocities rather than obtaining Manning's n values to compute stream velocities. To reduce client costs, we must be conscious of the information that is available and not redo computations where they are not warranted.

Fig. 12 — This figure is excellent. It should probably be expanded to include the months of May and October.

p.39, Par.3 — We suggest that AEIDC discontinue its literature search for techniques to improve the resolution of the (ground temperature) model.

p.40, Par.2 — Is the Talkeetna climate station representative of conditions further north in the basin? Presumably Fig. 19 is a comparison of monthly observed versus predicted which appears to be a good comparison. However, Fig. 19 does not show the comparison of Talkeetna temperatures with other basin temperatures. Thus, if Talkeetna data are to be used in the model, are they representative of basin conditions?

p.41, Bottom — Since monthly average wind speeds are used in the model, we fail to see the justification for obtaining wind speeds directly over the water surface. We could understand this for a lake,but for a river?

p.44 — Top figure. Is the value (9.3°C predicted, 2°C observed) for Watana correct?

p.45,46 — There appears to be something seriously wrong here. We believe more work is necessary to understand what the problem is. For example, how do the observed relative humidities at the stations compare with one another?

p.51-54

The predicted temperatures in Appendix C generally indicate increasing temperature with distance downstream except for the Chulitna confluence. We are not convinced that the observed data show this. Thus, can we say the model is calibrated? To apply the model to postproject conditions may not be valid.

p.55 Future Applications

1) Normal and extreme flow regimes for the 32-year record should be defined in coordination with H-E. (See general comments).

2) Please explain what is meant by "This will identify the area facing possible hydrologic/hydraulic impacts?"

3) Good, but do in coordination with H-E,as this is necessary for other models.

8) Techniques for improving the groundwater temperature should not be pursued at this time.

Part a:

AEIPC's

Response

to

General Comments

SUS # 218

RESPONSE TO GENERAL COMMENTS

We feel that, although the AEIDC report entitled "Stream Flow and Temperature Modeling in the Susitna Basin, Alaska" is written for a technical audience, a detailed description of the SNTEMP model would be unnecessary since the temperature model description is available from the Instream Flow Group, U.S. Fish and Wildlife Service (the reference Theurer et al. 1983 in the draft report). The description is lengthy and its inclusion in the AEIDC report would detract from the purpose of the report: a description of the modifications of the stream temperature model, the techniques used for data genesis, and the methods employed for validation and calibration. Attachment 1 of this memo is a copy of the mathematical model description from a draft of the Theurer et al. 1983 paper which we hope will be useful in providing background to the AEIDC report.

The decision to investigate other methods of determining subbasin flow contributions was made at a March 15, 1983, meeting between Harza-Ebasco and AEIDC personnel. We agreed then to examine more sophisticated approaches which included the effects of precipitation distribution, and to respond in a letter report to Dr. B.K. Lee in April.

The decision to test the three weighting methods using a large set of subbasins rather than one or two individual subbasins was based on a number of reasons. The resolution of the precipitation and water yield distribution maps used to determine weighting coefficients are low enough to allow substantial miscalculation of coefficients for any single subbasin. By testing on a composite set of subbasins, higher basinwide accuracy would be expected. Additionally the largest set of flow data available to test these coefficients was on the mainstem river rather than on individual tributaries.

This is important as the weighting coefficients were derived from maps representing average trends; anomalous runoff events on small subbasins could easily lead to unrepresentative short-term flow records. Finally, delineation and planimetry of all subbasins was necessary for watershed area weighting. Once this and the additional work transferring precipitation and water yield isopleths onto the base map was done, little extra time was required to calculate water yield and precipitation coefficients for all subbasins.

As described later in this memo, alternate techniques could be used in predicting tributary temperatures. The technique chosen should be physically based to insure reasonable predictions when the model is used to extrapolate tributary temperatures. We have discovered that the tributaries have a major influence on the mainstem temperature in simulations of postproject conditions. We also feel that accurate tributary temperature predictions may be necessary to address thermal shock effects on spawners traveling from the mainstem into the tributaries.

We are presently organizing the data necessary to simulate daily stream temperatures. Our initial effort will be validation of the stream temperature model predictions using 1982 data. A coordinated approach will be necessary for determining which periods should be simulated and for defining the purpose of daily simulations.

RESPONSE TO SPECIFIC COMMENTS

p. 1, para. 2 — Note that ADF&G and USFWS have undertaken studies of temperature effects on salmonid egg incubation.

The introduction to this temperature report paper was not intended to be all inclusive concerning the literature on temperature effects on the various fish life stages. We are aware of the studies being done by ADF&G and USFWS. Their respective reports are due out during the month of August 1983 and we will utilize the information as it becomes available.

p. 3, Par. 1 and p. 11, Par. 2

Since subjectiveness is involved in areal precipitation weighting (method 2), is using this method more appropriate than using the drainage area method?

Since Method (2) yields a higher Watana discharge, we recommend this method not be used at this time. The high discharge implies additional economic benefits. For economic runs, we need to be conservative. However, a final decision on the selected method will be made by H/E in the near future.

The subjectiveness of the precipitation weighting coefficients is due both to the methods used to arrive at those coefficients from the precipitation distribution map, and to the inherent "art" involved in developing that isohyetal map from the paucity of data available for the Susitna basin. Method 2 was chosen solely on the merit of its better agreement in predicting Watana streamflows than the other two methods. We think this method has merit and could be improved by refining the basin isohyetal map with the additional data that is being collected.

However, in the short term, we agree that the simpler drainage area method can be used. It should be clarified, though, that no matter which method is used, we have been running SNTEMP using the available monthly data sets provided in Exhibit E (ACRES 1983) (with the exception of the Sunshine data set). Flows at Watana (or at Devil Canyon for the two-dam scenario) and at Gold Creek are input to the water balance program, and are thus consistent with those used by ACRES and Harza-Ebasco. It is only the apportionment of water <u>between</u> gage sites that differs between these methods.

p. 9, Fig. 3 — Mean annual water yield for several subbasins appears to be greater than the mean annual precipitation (Tsusena, Fog, Devil, Chin-Chee, Portage).

This is true. Mean annual precipitation values were developed using the map of Wise (1977), and mean annual water-yield values using the map of Evan Merril of the Soil Conservation Service (1982). These numbers are clearly in dispute. This figure was included to demonstrate the differences between those weighting methods.

p. 10, Bottom — Calculated C_w for Method (1) is 0.5104. ACRES used 0.515. Why is there a difference? Were these areas replanimetered?

The basin between Cantwell and Gold Creek was divided into ten subbasins (Clarence through Indian, Figure 4 of the draft report), four upstream from the Watana dam site, and six downstream. The area of each subbasin was found by planimetry; the areas of the basin above and the basin below Watana were arrived at by summing the appropriate subbasin areas. Discrepancies in basin area measurements are expected when those basins are delineated and planimetered independently. Moreover, our procedure incorporates possible errors from a number of individual planimetry measurements, and compounding errors can occur. However, the agreement of these two figures is to less than one-half percent (0.0046) of the area between Cantwell and Gold Creek. This difference corresponds to an area less than 9 mi^2 in a watershed (defined at Watana) larger than 5000 mi^2.

Once again and most importantly, these coefficients are defined for the Cantwell to Gold Creek basin. When running SNTEMP, only the flow apportionment between basin sites having input data is affected. Thus mainstem flows at Watana, Gold Creek and Susitna Station are consistent with those flows used by other groups.

p. 18, Par. 1 We suggest using solar radiation measurements when available rather than calculated values. We would also like to see daily comparisons of observed versus computed solar radiation. Please provide descriptions of the six SNTEMP submodels.

We have decided to use predicted solar radiation rather than observed values so that we would be able to simulate water temperatures for periods when there was no data collected. This is useful for predicting average and extreme conditions which did not necessarily occur during the 1980 to 1982 periods. We have made an effort to calibrate the solar model to observed solar radiation data to make our predictions as representative as possible.

As Figure 22 indicates predicted solar radiation values are representative of basin for monthly average conditions. This figure demonstrates a tendency to overpredict Watana and underpredict Devil Canyon insolations. Thus, the solar model is predicting an average basin insolation. Since the current implementation of SNTEMP allows for only one meteorological data station, basin average solar radiations would have to be estimated from alternative means or area weighted averages. The solar model essentially averages conditions for us.

Calculated solar radiation is also necessary for simulating topographic shade effects. The solar model tracks the sun during the day and accounts for the time the stream surface is in shade due to the adjacent topography.

We will produce a plot similar to Figure 22 but with daily values if it becomes necessary to predict daily water temperatures.

Attachment 1 contains pertinent pages from the paper by Theurer et al. (1983) which describes the six SNTEMP submodels. These pages will be useful in clarifying some of the comments to other sections of AEIDC's draft flow and temperature report.

p. 19, Bottom — More discussion on heat flux would be helpful. Statements regarding the relative importance of heat inputs and outputs should be made. Please provide all heat sources and sinks considered.

Attachment 1 discussed in the previous response should clarify how the heat flux components (atmospheric, topographic, and vegetative radiation; solar radiation; evaporation; free and forced convection; stream friction; stream bed conduction; and water back radiation) are simulated by SNTEMP. We are working on a graphic presentation to demonstrate the values of the individual heat flux components for average monthly conditions but do not feel it will be available for the final version of this report. Preliminary plots of the heat flux components are presented in Attachment 2. The relatively high friction heat input is interesting and will probably be a major influence in fall and winter simulations.

p. 20 — In Eq. (9), how was T_e (Equilibrium temperature) estimated? What are the parameter values of K_1 and K_2?

The values of the equilibrium temperature (T_e) and 1st (K_1) and 2nd (K_2) thermal exchange coefficients are computed within SNTEMP. To visualize

the technique used, it is necessary to realize that the net heat flux (ΣH) is an analytical but nonlinear function of the stream temperature (due to the back radiation, evaporation, and convection heat components); i.e. $\Sigma H = f(T_w)$ where T_w is stream temperature. When stream temperature equals equilibrium temperature, the net heat flux is zero ($\Sigma H = f(T_w = T_e) = 0$). Newton's method is used to iterate to the equilibrium temperature with the air temperature being the initial estimate of T_e. The values for K_1 and K_2 follow since the first and second derivations of the heat flux are also analytical functions and:

$$\frac{d(\Sigma H)}{dT_w} = \frac{df_{K_1}}{dT_w}, \quad \frac{df_{K_2}}{dT_w} \Bigg|_{T_w = T_e} = K_1$$

$$\frac{d^2(\Sigma H)}{dT_w^2} = \frac{d^2 f_{K_2}}{dT_w^2}, \quad \frac{d^2 f_{K_2}}{dT_w^2} \Bigg|_{T_w = T_e} = K_2$$

Average values of T_e, K_1, and K_2 will be presented in a subsequent report which will include 1983 data/SNTEMP simulation validation.

p.21 There are potential problems with using temperature lapse rates at Fairbanks and Anchorage. Both sites are subject to temperature inversions because of topography. This may not occur along the Susitna River. We recommend that the existing Weather Wizard data be reviewed.

No long term upper air data are available for Talkeetna. Anchorage and Fairbanks vertical temperature (and humidity) data averaged over a six-year period (1968, 1969, 1970, 1980, 1981, and 1982) are felt to be the best available representation of vertical air temperature profiles for the Susitna River basin. Examination of numerous winter daily synoptic weather maps for surface, 850 mb, and 500 mb levels verifies the assumption that inversion strength and thickness in the Susitna River basin are roughly halfway between those observed in Anchorage and Fairbanks.

The Susitna basin is surrounded by mountains on the north, east and west. To the south it is open to the Cook Inlet and Gulf of Alaska. In winter, the Alaska range blocks most low level interior air from reaching and influencing the Susitna basin and Anchorage. However, radiative processes in concert with topography are responsible for producing a strong, well documented low level inversion in the Susitna valley (Comiskey, pers. comm.). This inversion is not as severe as in Fairbanks, but more severe than in Anchorage. Data from both stations are retained since upper air temperatures for all three regions are relatively uniform.

Topographic variability will introduce local systematic error in the vertical profiles. Cold air flows downhill where radiative cooling in the valleys further reduces air temperatures. Weather Wizard data gathered at stations within the basin may reflect highly localized weather activity. Within the mountain walls vertical and lateral air mass extent and movement is limited compared to that of the synoptic scale events governing the major air mass properties. Local topographic effects cannot be reliably incorporated into the larger scale vertical lapse rate regime.

This strong inversion is not just a statewide phenomena, but occurs throughout the high latitudes in winter. Due to the small heat capacity of the land surface its temperature is highly dependent upon absorption of solar radiation. Minimal radiation is absorbed in Alaska (i.e., the Susitna River basin) in winter for the following four reasons: (1) a high albedo, (2) short hours of daylight, (3) the oblique angle of the sun's rays, and (4) screening by clouds of ultraviolet rays. Consequently, a warm maritime air mass flowing from the North Pacific or Bering Sea over Alaska will be strongly cooled at the earth's surface. When subsequent air masses move onshore they are forced to flow aloft by the previously cooled, dense stable surface layer. Daytime heating at the earth's surface is usually not strong enough to destroy the inversion. Over a 24-hour cycle no well-defined mixed layer remains and fluxes of latent and sensible heat are very small. The inversion's longevity is enhanced when the wind speeds are low and corresponding momentum transfer is weak. Talkeetna is typified by comparatively low average wind speeds, on the order of 5 mph during the winter months. A single strong wind event can disperse the inversion temporarily; however, it will occur frequently each winter and is considered a semi-permanent feature.

Translocating average temperature profiles from Anchorage and Fairbanks in the spring, summer, and fall to the Susitna River basin is well within acceptable limits. The temperature profiles generated by this method fall precisely within the moist adiabatic lapse rate, as predicted by standard theory. The temperature data gathered from upper air National Weather Service radiosonde instruments is highly correlated with temperatures measured in the basin by the Weather Wizard. This argument further substantiates use of large scale data to predict local temperature patterns.

p.24, Par. 4 — How have we demonstrated that topographic shading has an important influence on the Susitna River? While we do not dispute this, we would like to see this verified with a sensitivity run.

Our statement is in error since we have not demonstrated that topographic shading has an important influence on Susitna stream temperatures. Initial sensitivity simulations without topographic shade have shown that the corresponding increase in solar radiation has only a small effect on the stream temperatures. The significance of the shade effects has only been tested for average natural June through September conditions where an increase of less than 0.2 C was simulated without shade from Cantwell to Sunshine. Based on the solar path plots in Appendix A of the draft report, we would expect that the shading effects in other months would be greater but still relatively small. The wording of this paragraph will be changed to reflect the new knowledge gained from this sensitivity study.

p. 27, Par. 2 — Stream surface area is necessary to compute heat flux. According to Figure 26, we are considering only ten (10) reaches. How representative are these reaches for determining stream width and hence surface areas for the river segment between Watana and Sunshine? While Appendix B illustrates the representativeness of the ten (10) reacnes, it appears that we may have lost some of the refinement of the Acres model with its approximately sixty (60) reaches.

We feel that increasing the number of simulated reaches would improve the representativeness of the stream temperature model as would any increase in data detail. Based on our familiarity with SNTEMP, we did not originally feel that this many reaches were necessary. Nevertheless, we can increase the number of reaches for simulation purposes; the data is already available and the only increase in the client's costs will be the manpower to add them to SNTEMP data files and the increased computational time.

We are not familiar with the ACRES stream temperature model and do not know the model's stream width or hydraulic data requirements.

p. 29, Par. 1 To compute daily minimum and maximum tmperatures, we suggest the use of HEC-2 velocities rather than obtaining Manning's n values to compute stream velocities. To reduce client costs, we must be conscious of the information that is available and not redo computations where they are not warranted.

There would be two objections to using HEC-2 velocities as input to SNTEMP: (1) HEC-2 simulations would be required for all water temperature simulations where the minimum and maximum water temperatures were desired; and (2) SNTEMP would have to be modified to accept velocities.

Velocity input is not currently necessary to run SNTEMP for minimum and maximum temperatures since it is computed internally. This allows us to use SNTEMP for simulating any ice-free period from 1968 to 1982 (or later, when the required data are received). Thus, we can determine the extreme meteorological/flow periods for simulating maximum and minimum average daily temperatures and the diurnal variation around these extreme daily temperatures. If the HEC-2 velocity estimates are required, this flexibility would be lost. If the Susitna Aquatic Impact Study Team could agree on the periods for minimum and maximum temperature predictions, this first problem could be eliminated.

Modifying SNTEMP to accept velocities, however, would be a major undertaking. The explanation for this would be lengthy; we would prefer to discuss this potential modification at a technical meeting to explain the amount of work necessary and to help decide if SNTEMP should be modified or alternate techniques used.

Figure 12 — This figure is excellent. It should probably be expanded to include the months of May and October.

We agree that Figure 12 is both useful and usable and should be expanded to include May and October data as well as 1983 data. However, due to budgetary and time constraints, we will not be able to revise this figure until after the October 14 report.

p. 39, Par 3 — We suggest that AEIDC discontinue its literature search for techniques to improve the resolution of the (ground temperature) model.

This is not an intensive literature search. We are limiting our search to the journals and reports we normally read within the course of our professional maintenance and to conversations with other professionals who may have experience and knowledge of lateral flows and temperature in general and Susitna conditions specifically. The last sentence of this paragraph will be replaced with "AEIDC believes this model currently provides the best available approximation of the physical conditions existing in the Susitna basin and will be applied without validation until better estimates of existing conditions are obtained."

p. 40, Par 2 — Is the Talkeetna climate station representative of conditions further north in the basin? Presumably Fig. 19 is a comparison of monthly observed versus precicted which appears to be a good comparison. However, Fig. 19 does not show the comparison of Talkeetna temperatures with other basin temperatures. Thus, if Talkeetna data are to be used in the model, are they representative of basin conditions?

Talkeetna climate data would not be representative of conditions within the basin if applied without adjustment. The last two sentences of this paragraph will be changed to "This period of record allows stream temperature simulations under extreme and normal meteorology once these data are adjusted to better represent conditions throughout the Susitna basin. We used meteorologic data collected specifically for the Susitna study to validate this meteorologic adjustment and the solar model predictions." We hope this will clarify that we are not blindly applying Talkeetna data without adjustment.

Apparently Figure 19 has been misunderstood. The predicted temperatures are based on observed temperatures at Talkeetna and the lapse rates which we have developed (Figure 7 in the report). Given the observed temperature at the Talkeetna elevation, the lapse rate equations are used to predict temperatures at any elevation. The air temperatures predicted for the elevations of the Sherman, Devil Canyon, Watana, and Kosina Weather Wizards were compared to the air temperatures observed by R&M (Figure 19 in the report).

p. 41, Bottom — Since monthly average wind speeds are used in the model, we fail to see the justification for obtaining wind speeds directly over the water surface. We could understand this for a lake, but for a river?

As Figure 21 suggests, the wind speed data collected at Talkeetna represents average basin winds as collected at the four R&M sites (at least the data at Talkeetna is not extremely different). What these wind speed data represent, however, is not fully understood. The evaporative and convective heat flux is driven by local (2 m above the water surface) wind speeds. The Watana, Devil Canyon, and Kosina stations are located high above the water

surface (as we understand, we have not visited the sites). This implies that the data collected do not meet the model's requirements; however, we agree that it is not necessary to collect additional data if this would be very expensive. In our initial conversation with Jeff Coffin of R&M Consultants, we inquired if it would be possible to obtain this data easily as part of their existing collection effort. He felt it would be possible. A return call from Steve Bredthauer informed us that equipment necessary to collect this data was not available and would have to be purchased. Our response was that this data would improve our understanding of in-canyon winds but would not be necessary at the expense envisioned. We have replaced this last sentence on Page 41 with "Since it appears to be impractical to collect wind speed data within the canyons below the existing meteorological data sites (Bredthauer 1983), the wind speed data collected at Talkeetna will be used as representative of average basin winds."

p. 44 Top figure. Is the value (9.3° C predicted, 2° C observed) for Watana correct?

SNTEMP did predict an air temperature of 9.3 C and an average air temperature of 2 C was observed for August 1981 at the Watana weather station. The observed Watana data is obviously in error (e.g., a temperature of -30.9 C was recorded for 15 August 1981) and probably should not have been included for validation of the air temperature lapse model in this plot. As stated in the report, none of the Weather Wizard data were used in the water temperature simulations but are presented as a validation of the adjustment of the observed Talkeetna data. Careful review of the Weather Wizard data (especially humidities) would be necessary if these data were to be used in

water temperature simulations. This data point will be removed from the plot in the final draft.

p. 45, 46 There appears to be something seriously wrong here. We believe more work is necessary to understand what the problem is. For example, how do the observed relative humidities at the stations compare with one another?

The large variability in observed Weather Wizard data gives rise to doubts of its reliability. Data which are smoothed by monthly averaging are not expected to exhibit the year to year range of humidities which was observed at the Weather Wizard stations. The entire data set is characterized by irregular large annual changes in average relative humidities on the order of 30% to 40%. Talkeetna relative humidity values, measured by the National Weather Service, are consistently greater by approximately 20% throughout the data. Talkeetna values are in agreement with the large scale picture generated by averaged Anchorage and Fairbanks data. For this reason, and those enumerated on Page 41 in the draft report, AEIDC maintains that the predictive scheme derived for input into the stream temperature model is the best representation of relative humidity with height for input in the surface flux calculations.

Five sample figures from the R&M raw data are presented for inspection (Attachment 3). Figures 1 and 2 present summer (June 1981) and winter (November 1980) situations where the correlation between Weather Wizard data at two stations is illustrated. In both instances the relative humidity data is in good agreement from one station to another. These were chosen as exemplary months; they are not, however, typical. Figure 3 indicates two common errors, missing days of data and an unvarying upper limit. Another common error discussed in the report is illustrated by Figure 4. Erratic

daily swings from zero to 100 percent exist throughout the data. Figure 5 illustrates simultaneous comparison of Watana Weather Wizard data and surface relative humidities measured at Talkeetna by the National Weather Service. The correlation between the two is poor.

Attempts to explain the erratic swings in the data (daily, monthly and annually) as highly localized topographic or microscale weather events is also unsatisfactory. Over time, monthly averaging would smooth anomalies. However, a three-year average for each month still retains a high variability with elevation (see Figure 6, Attachment 3). From year to year topography requires that highly localized atmospheric events be fairly consistent, thereby giving rise to identifiable trends in the data. Such is not the case. AEIDC meteorologists concur that instrument calibration problems are the probable explanation for the high variability in the data.

The best way to verify these conclusions regarding the reliability of the relative humidity data collected in the Susitna basin would be to perform a spot calibration of the Weather Wizards. A wet bulb-dry dry bulb sling psychrometer could be carried to the remote weather stations where the relative humidities measured by each method can be compared.

p. 51-54 The predicted temperatures in Appendix C generally indicate increasing temperature with distance downstream except for the Chulitna confluence. We are not convinced that the observed data show this. Thus, can we say the model is calibrated? To apply the model to postproject conditions may not be valid.

We have some problems in believing the observed data, especially the variation in downstream temperatures observed in August 1981, September 1981, and August 1982. We do not understand what would cause the types of variations indicated unless there were tributary impacts which we were not

considering. We feel, however, that we have made a thorough attempt at modeling tributary flows and temperatures.

We are not thoroughly familiar with the techniques used by ADF&G to verify and calibrate their thermographs. Their techniques are not published in any Susitna reports.

We recommend that data verification be performed. Wayne Dyok, H-E, has collected some longitudinal temperature data which tends to support the downstream increase in temperature which we have predicted. Wayne's effort was helpful but does not identify which thermographs or data sets may be in error. Until faulty data sets are identified (if any) we do not feel we should attempt to increase the degree of fit of the model.

As to applying the model to postproject conditions, we feel that, at the very least, it is necessary that some initial estimates of project impacts be made at this time. It may be necessary to label these simulations as preliminary results until temperature data is verified.

p. 55, Future Applications

1) Normal and extreme flow regimes for the 32-year record should be defined in coordination with H-E. (See general comments).

Our intent here is to identify the natural range of flow regimes in the Susitna basin, not to necessarily "define" representative flow years for more detailed study. We agree that identifying such years should be done by AEIDC and H-E together, insuring the most thorough results for the efforts of each.

p. 55

2) Please explain what is meant by "This will identify the area facing possible hydrologic/hydraulic impacts?"

If possible, we will determine the location downstream from the project where operational flows become statistically indistinguishable from natural flows. This will vary on a month-by-month basis. If project flows downstream from a given location are insignificantly different from natural flows, we reason that flow-related impacts must also be indistinguishable, and, therefore, need not be examined further.

p. 55 3) Good, but do in coordination with H-E, as this is necessary for other models.

We have met with Wayne Dyok of Harza-Ebasco and discussed our approach in simulating normal and extreme stream temperature changes. The periods we selected were not the same as the periods selected by Harza-Ebasco. Since we had a deadline to meet in producing a stream temperature effects paper, there was insufficient time for a more coordinated approach. We feel that more coordination will be of mutual benefit in the future.

p. 55 8) Techniques for improving the groundwater temperature should not be pursued at this time.

We have found that the influence of the tributaries on the mainstem is significant, especially in postproject simulations. The distributed flow temperature model was developed to improve the tributary temperature predictions with a physically reasonable model. There are other approaches to predicting tributary temperatures but the technique used will have to meet several requirements: (1) it must be general enough to apply to June-September periods without observed tributary temperatures, (2) it must be applicable to winter conditions for future ice simulations, and (3) any technique used cannot depend on more data than is available. The technique which you have

suggested (relating tributary temperatures to air temperatures) may be possible when the 1983 field data becomes available, although we would recommend a regression model based on computed equilibrium temperatures. There is not enough monthly tributary data currently available for any regression approach. Daily air temperature and tributary temperature data suggests a correlation (Attachment 4 is a scattergram of recorded Indian River temperatures versus air temperatures) but we believe that a regression model based on daily data would result in a tributary temperature model which would not be as capable as the distributed flow temperature model.

As you request, we will not pursue techniques for improving the distributed flow temperature model at this time. This model will be used as is for all simulations until the 1983 tributary temperature data becomes available. When the 1983 data are available, we will look at possible regression models for predicting tributary temperatures. We will then select the best approach. Harza-Ebasco's involvement in this selection process would be appreciated.

Attachment 1

SNTEMP MATHEMATICAL MODEL DESCRIPTION

INTRODUCTION

This part is to explain each of the physical processes affecting instream water temperatures and their mathematical descriptions so that the responsible engineer/scientist can understand the behavior of the model. It will enable the responsible engineer/scientist to determine the applicability of the model, the utility of linking the model with other models, and the validity of results.

The instream water temperature model incorporates: (1) a complete solar model including both topographic and riparian vegetation shade; (2) an adiabatic meteorological correction model to account for the change in air temperature, relative humidity, and atmospheric pressure as a function of elevation; (3) a complete set of heat flux components to account for all significant heat sources; (4) a heat transport model to determine longitudinal water temperature changes; (5) regression models to smooth or complete known water temperature data sets at measured points for starting or interior validation/calibration temperatures; (6) a flow mixing model at tributary junctions; and (7) calibration models to eliminate bias and/or reduce the probable errors at interior calibration nodes.

SOLAR RADIATION

The solar radiation model has four parts: (1) extra-terrestrial radiation, (2) correction for atmospheric conditions, (3) correction for cloud cover, and (4) correction for reflection from water surface. The extra-terrestrial radiation, when corrected for both the atmosphere and cloud cover, predicts the average daily solar radiation received at the ground on a horizontal surface of unit area. Therefore, it is the total amount of solar energy per unit area that projects onto a level surface in a 24-hour period. It is expressed as a constant rate of heat energy flux over a 24-hour period even though there is no sunshine at night and the actual solar radiation varies from zero at sunrise and sunset to a maximum intensity at solar noon.

EXTRA-TERRESTRIAL RADIATION

The extra-terrestrial radiation at a site is a function of the latitude, general topographic features, and time of year. The general topographic features affect the actual time of sunrise and sunset at a site. Therefore, the effect of solar shading due to hills and canyon walls can be measured. The time of year directly predicts the angle of the sun above or below the equator (declination) and the distance between the earth and the sun (orbital position). The latitude is a measure of the angle between horizontal surfaces along the same longitude at the equator and the site.

The extra-terrestrial solar radiation equation is

$$H_{sx,i} = (q_s/\pi)\ \{[(1 + e\cos\theta_i)^2/(1-e^2)]\} \qquad (\ )$$

$$\{[h_{s,i}(\sin\phi\ \sin\delta_i)] + [\sinh_{s,i}(\cos\phi\ \cos\delta_i)]\}$$

where:

q_s ≡ solar constant = 1377, J/m²/sec.

e ≡ orbital eccentricity = 0.0167238, dimensionless.

θ_i ≡ earth orbit position about the sun, radians.

ϕ ≡ site latitude for day i, radians.

δ_i ≡ sun declination for day i, radians.

$h_{s,i}$ ≡ sunrise/sunset hour angle for day i, radians.

$H_{sx,i}$ ≡ average daily extra-terrestrial solar radiation for day i, J/m²/sec.

The extra-terrestrial solar radiation may be averaged over any time period according to

$$\bar{H}_{sx} = \left[\sum_{i=n}^{N} H_{sx,i}\right]/[N-n+1] \qquad (\ )$$

where:

$H_{sx,i}$ ≡ extra-terrestrial solar radiation for day i, J/m²/sec.

N ≡ last day in time period, Julian days.

n ≡ first day in time period, Julian days.

i ≡ day counter, Julian days.

$\bar{H}_{sx}$ ≡ extra-terrestrial solar radiation averaged over time period n to N, J/m²/sec.

The earth orbit position and sun declination as a function of the day of year are

$$\theta_i = [(2\pi/365)\ (D_i-2)] \qquad (\ )$$

$$\delta_i = 0.40928 \cos [(2\pi/365)\ (172-D_i)] \qquad (\ )$$

where: $D_i \equiv$ day of year, Julian days; $D_i=1$ for January 1 and $D_i=365$ for December 31.

$\theta_i \equiv$ earth orbit position for day i, Julian days.

$\delta_i \equiv$ sun declination for day i, Julian days.

The sunrise/sunset hour angle is a measure of time, expressed as an angle, between solar noon and sunrise/sunset. Solar noon is when the sun is at its zenith. The time from sunrise to noon is equal to the time from noon to sunset only for symeterical topographic situations. However, for simplicity, this model will assume that an average of the solar attitudes at sunrise/sunset is used. Therefore, the sunrise/sunset hour angle is

$$h_{s,i} = \arccos \{[\sin\alpha_s - (\sin\phi\ \sin\delta_i)]/[\cos\phi\ \cos\delta_i]\} \qquad (\ )$$

$$\bar{h}_s = [\sum_{i=n}^{N} h_{s,i}]/[N-n+1] \qquad (\ )$$

where: $\phi \equiv$ site latitude, radians.

$\delta_i \equiv$ sun declination for day i, radians.

$\alpha_s \equiv$ average solar altitude at sunrise/sunset, radians; $\alpha_s = 0$ for flat terrian, $\alpha_s > 0$ for hilly or canyon terrian.

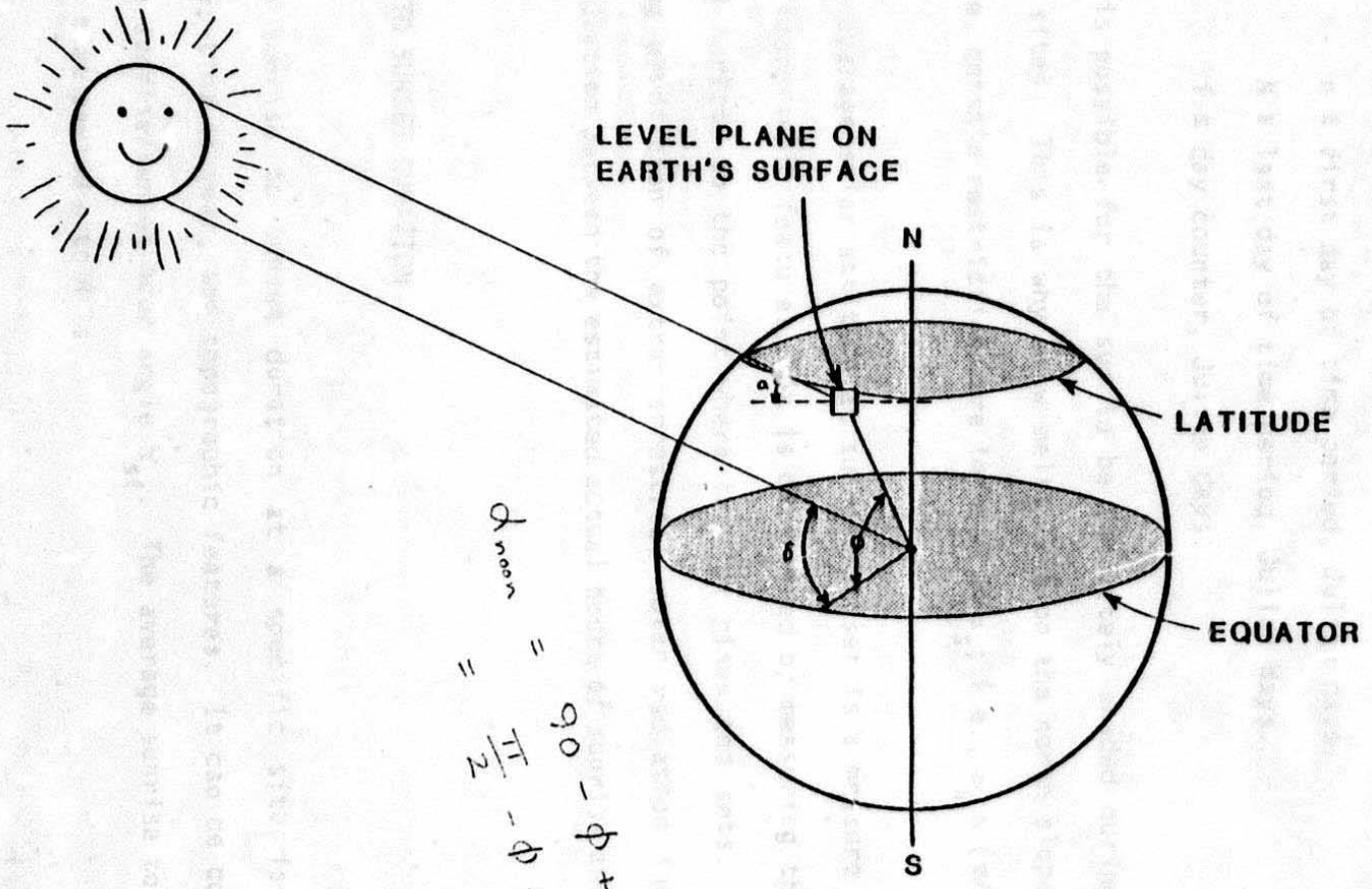

Figure 2.1. Solar angular measurements.

$h_{s,i}$ ≡ sunrise/sunset hour angle for day i, radians

$\bar{h}_s$ ≡ average sunrise/sunset hour angle over the time period n to N, radians.

n ≡ first day of time period, Julian days.

N ≡ last day of time period, Julian days.

i ≡ day counter, Julian days.

It is possible for the sun to be completely shaded during winter months at some sites. This is why snow melts last on the north slopes of hillsides. Therefore, certain restrictions are imposed on α_s; i.e., $\alpha_s \leq (\pi/2) - \phi + \delta_i$.

The average solar attitude at sunrise/sunset is a measure of the obstruction of topographic features. It is determined by measuring the average angle from the horizon to the point where the sun rises and sets. Therefore, the resulting prediction of extra-terrestrial solar radiation includes only the solar radiation between the estimated actual hours of sunrise and sunset.

SUNRISE TO SUNSET DURATION

The sunrise to sunset duration at a specific site is a function of latitude, time of year, and topographic features. It can be computed directly from the sunrise/sunset hour angle h_{si}. The average sunrise to sunset duration over the time period n to N is

$$S_o = (12/\pi)\ \bar{h}_s \qquad (\ )$$

where: $S_o \equiv$ average sunrise to sunset duration at the specific site over the time period n to N, hours.

$\bar{h}_s \equiv$ average sunrise/sunset hour angle over the time period n to N, radians.

ATMOSPHERIC CORRECTION

The extra-terrestrial solar radiation is attenuated on its path through the atmosphere by scattering and absorbtion when encountering gas molecules, water vapor, and dust particles. Furthermore, radiation is reflected from the ground back into the sky where it is again scattered and reflected back again to the ground.

The attenuation of solar radiation due to the atmosphere can be approximated by Beer's law

$$H_{sa} = (e^{-\eta z})\, H_{sx} \qquad (\ )$$

where: $H_{sx} \equiv$ average daily extra-terrestrial solar radiation; $J/m^2/sec.$

$H_{sa} \equiv$ average daily solar radiation corrected for atmosphere only, $J/m^2/sec.$

$\eta \equiv$ absorbtion coefficient, 1/m.

$z \equiv$ path length, m.

While Beer's law is valid only for monochromatic radiation, it is useful to predict the form of and significant variables for the atmospheric correction equation. Repeated use of Beer's law and recognition of the importance of the

optical air mass (path length), atmospheric moisture content (water vapor), dust particles, and ground reflectivity results in a useful emperical atmospheric correction approximation.

$$e^{-\eta z} = [a'' + (1-a'-d)/2]/[1-R_g(1-a'+d)/2] \qquad (\ )$$

where: a' ≡ mean atmospheric transmission coefficient for dust free moist air after scattering only, dimensionless.

a'' ≡ mean distance transmission coefficient for dust free moist air after scattering and absorbiton; dimensionless.

d ≡ total depletion coefficient of the direct solar radiation by scattering and absorbtion due to dust, dimensionless.

R_g ≡ total reflectivity of the ground in the vicinity of the site, dimensionless.

The two transmission coefficients may be calculated by

$$a' = \exp\{-[0.465 + 0.134\ w]\ [0.129 + 0.171 \exp(-0.880\ m_p)]\ m_p\} \qquad (\ )$$

$$a'' = \exp\{-[0.465 + 0.134\ w]\ [0.179 + 0.421 \exp(-0.721\ m_p)]\ m_p\} \qquad (\ )$$

where: w ≡ precipitable water content, cm.

m_p ≡ optical air mass, dimensionless.

The precipitable water content, w, of the atmosphere can be obtained using the following pair of formulas.

$$(1.0640^{T_d})/(T_d+273.16) = (R_h 1.0640^{T_a})/(T_a+273.16) \qquad (\ )$$

$$w = 0.85 \exp(0.110 + 0.0614\ T_d) \qquad (\ )$$

where: $T_a \equiv$ average daily air temperature, C.

$R_h \equiv$ relative humidity, dimensionless.

$T_d \equiv$ mean dew point, C.

$w \equiv$ precipitable water content, cm.

The optical air mass is the measure of both the path length and absorbtion coefficient of a dust-free dry atmosphere. It is a function of the site elevation and instantaneous solar altitude. The solar altitude varies according to the latitude of the site, time of year, and time of day. For practical application, the optical air mass can be time-averaged over the same time period as the extra-terrestrial solar radiation. The solar altitude function is

$$\alpha_i = \arcsin \{[\sin\phi \sin\delta_i] + [\cos\phi \cos\delta_i)]\} \quad (\ )$$

$$\bar{\alpha} = \{ \sum_{i=n}^{N} [(\int_o^{h_{s,i}} \alpha_i \, dh)/h_{s,i}]\}/[N-n+1] \quad (\ )$$

where: $\phi \equiv$ site latitude, radians.

$\delta_i \equiv$ sun declination on day i, radians.

$h \equiv$ instantaneous hour angle, radians.

$h_{s,i} \equiv$ sunrise/sunset hour angle for day i, radians.

$n \equiv$ first day in time period, Julian days.

$N \equiv$ last day in time period, Julian days.

$i \equiv$ day counter, Julian days.

$\alpha_i \equiv$ instantaneous solar altitude during day i, radians.

$\bar{\alpha} \equiv$ average solar altitude over time period n to N, radians.

Equation A14 can be solved by numerical integration to obtain a precise solution. However, if the time periods do not exceed a month, a reasonable approximation to the solution is

$$\tilde{\alpha}_i = \arcsin \{[\sin\phi \sin\delta_i] + [\cos\phi \cos\delta_i \cos (h_{s,i}/2)]\} \quad (\ )$$

$$\bar{\alpha} = [\sum_{i=n}^{N} \tilde{\alpha}_i]/[N-n+1] \quad (\ )$$

where: $\tilde{\alpha}_i \equiv$ average solar altitude during day i, radians.

remaining parameters as previously defined.

The corresponding optical air mass is

$$m_p = \{[(288-0.0065Z)/288]^{5.256}\}/\{\sin \bar{\alpha} + 0.15[(180/\pi)\bar{\alpha} + 3.885]^{-1.253}\} \quad (\ )$$

where: $Z \equiv$ site elevation above mean sea level, m.

$\bar{\alpha} \equiv$ average solar altitude for time period n to N, radians.

$m_p \equiv$ average optical air mass, dimensionless.

The dust coefficient d and the ground reflectivity R_g may be estimated from Tables A1 and A2 respectively or they can be calibrated to published solar radiation data (Cinquemani et. al, 1978) after cloud cover corrections have been made.

Table A1. Dust coefficient d.[1]

Season	Washington, DC		Madison, Wisconsin		Lincoln, Nebraska	
	m_p=1	m_p=2	m_p=1	m_p=2	m_p=1	m_p=2
Winter	-	0.13	-	0.08	-	0.06
Spring	0.09	0.13	0.06	0.10	0.05	0.08
Summer	0.08	0.10	0.05	0.07	0.03	0.04
Fall	0.06	0.11	0.07	0.08	0.04	0.06

[1]Tennessee Valley Authority 1972, page 2.15.

Table A2. Ground reflectivity R_g.[2]

Ground condition	R_g
Meadows and fields	0.14
Leave and needle forest	0.07 - 0.09
Dark, extended mixed forest	0.045
Heath	0.10
Flat ground, grass covered	0.25 - 0.33
Flat ground, rock	0.12 - 0.15
Sand	0.18
Vegetation early summer leaves with high water content	0.19
Vegetation late summery leaves with low water content	0.29
Fresh snow	0.83
Old snow	0.42 - 0.70

[2]Tennesee Valley Authority 1972, page 2.15.

Seasonal variations appear to occur in both d and R_g. Such seasonal variations can be predicted resulting in reasonable estimates of ground solar radiation.

The dust coefficient d of the atmosphere can be seasonally distributed by the following empirical relationship.

$$d = d_1 + \{[d_2 - d_1] \sin [(2\pi/365) (D_i - 213)]\} \qquad (\ )$$

where: $d_1 \equiv$ minimum dust coefficient occurring in late July - early August, dimensionless.

$d_2 \equiv$ maximum dust coefficient occurring in late January - early February, dimensionless.

$D_i \equiv$ day of year, Julian days; D_i=1 for January 1 and D_i=365 for December 31.

The ground reflectivity R_g can be seasonally distributed by the following empirical relationship.

$$R_g = R_{g_1} + \{[R_{g_2} - R_{g_1}] \sin [(2\pi/365) (D_i - 244)\} \qquad (\ )$$

where: $R_{g_1} \equiv$ minimum ground reflectivity occurring in mid-September, dimensionless.

$R_{g_2} \equiv$ maximum ground reflectivity occurring in mid-March, dimensionless.

$D_i \equiv$ day of year, Julian days; D_i=1 for January 1 and D_i=365 for December 31.

The average minimum-maximum value for both the dust coefficient and ground reflectivities can be calibrated to actual recorded solar radiation data. Summaries of recorded solar radiation can be found in Cinquemani, et al. 1978.

CLOUD COVER CORRECTION

Cloud cover significantly reduces direct solar radiation and somewhat reduces diffused solar radiation. The preferred measure of the effect of cloud cover is the "percent possible sunshine" recorded value (S/S_o) as published by NOAA. It is a direct measurement of solar radiation duration.

$$H_{sg} = [0.22 + 0.78\ (S/S_o)^{2/3}]\ H_{sa} \qquad (\ )$$

where: $H_{sg} \equiv$ daily solar radiation at ground level.

$H_{sa} \equiv$ solar radiation corrected for atmosphere only.

$S \equiv$ actual sunshine duration on a cloudy day.

$S_o \equiv$ sunrise to sunset duration at the specific site.

If direct S/S_o values are not available, then S/S_o can be obtained from estimates of cloud cover C_ℓ.

$$S/S_o = 1 - C_\ell^{5/3} \qquad (\ )$$

where: $C_\ell \equiv$ cloud cover, dimensionless.

DIURNAL SOLAR RADIATION

Obviously, the solar radiation intensity varies throughout the 24-hour daily period. It is zero at night, increases from zero at sunrise to a maximum

at noon, and decreases to zero at sunset. This diurnal variation can be approximated by:

$$H_{nite} = 0 \qquad (\ )$$

$$H_{day} = (\pi/\bar{h}_s)\, H_{sg} \qquad (\ )$$

where: H_{nite} ≡ average nighttime solar radiation, J/m²/sec.

H_{day} ≡ average daytime solar radiation, J/m²/sec.

H_{sg} ≡ average daily solar radiation at ground level, J/m²/sec.

$\bar{h}_s$ ≡ average sunrise/sunset hour angle over the time period n to N, radians.

SOLAR RADIATION PENETRATING WATER

Solar or shortwave radiation can be reflected from a water surface. The relative amount of solar radiation reflected (R_t) is a function of the solar angle and the proportion of direct to diffused shortwave radiation. The average solar angle α is a measure of the angle and the percent possible sunshine S/S_o reflects the direct-diffused proportions.

$$R_t = A(S/S_o)\, [\bar{\alpha}(180/\pi)]^{B(S/S_o)}\ ;\ 0 \le R_t \le 0.99 \qquad (\ )$$

where: R_t ≡ solar-water reflectivity coefficient, dimensionless.

$\bar{\alpha}$ ≡ average solar altitude, radians.

$A(S/S_o)$ ≡ coefficient as a function of S/S_o.

$B(S/S_o)$ ≡ coefficient as a function of S/S_o.

S/S_o ≡ percent possible sunshine, dimensionless.

Both $A(S/S_o)$ and $B(S/S_o)$ are based on values given in Table 2.4 Tennessee Valley Authority, 1972. The following average high and low cloud values were selected from this table to fit the curves.

C_ℓ	S/S_o	A	A'	B	B'
0	1	1.18	-	-0.77	-
0.2	0.932	2.20	0	-0.97	0
1	0	0.33	-	-0.45	-

where: $A' = dA/dC_\ell$ and $B' = dB/dC_\ell$

The resulting curves are:

$$A(S/S_o) = [a_0 + a_1 (S/S_o) + a_2 (S/S_o)^2]/[1 + a_3(S/S_o)] \quad (\ )$$

$$B(S/S_o) = [b_0 + b_1 (S/S_o) + b_2 (S/S_o)^2]/[1 + b_3 (S/S_o)] \quad (\ )$$

where:

$a_0 = 0.3300$	$b_0 = -0.4500$
$a_1 = 1.8343$	$b_1 = -0.1593$
$a_2 = -2.1528$	$b_2 = 0.5986$
$a_3 = -0.9902$	$b_3 = -0.9862$

The amount of solar radiation actually penetrating an unshaded water surface is:

$$H_{sw} = (1-R_t)\, H_{sg} \quad (\ )$$

where: $H_{sw} \equiv$ daily solar radiation entering water, $J/m^2/sec$

$R_t \equiv$ solar-water reflectivity, dimensionless

$H_{sg} \equiv$ daily solar radiation at ground level, $J/m^2/sec$

SOLAR SHADE

The solar shade factor is a combination of topographic and riparian vegetation shading. It is a modifaction and extension of Quigley's (1981) work. It distinguishes between topographic and riparian vegetation shading, and does so for each side of the stream. It was modified to include the intensity of the solar radiation throughout the entire day and is completely consistent with the heat flux components used with the water temperature model.

Topographic shade dominates the shading effects because it determines the local time of sunrise and sunset. Riparian vegetation is important for shading between local sunrise and sunset only if it casts a shadow on the water surface.

Topographic shade is a function of the: (1) time of year, (2) stream reach latitutde, (3) general stream reach azimuth, and (4) topographic altitude angle. The riparian vegetation is a function of the topographic shade plus the riparian vegetation parameters of: (1) height of vegetation, (2) crown measurement, (3) vegetation offset, and (4) vegetation density. The model allows for different conditions on opposite sides of the stream.

The time of the year (D_i) and stream reach latitude (ϕ) parameters were explained as a part of the solar radiation section. The remaining shade parameters are peculiar to determination of the shading effects.

The general stream reach azimuth (A_r) is a measure of the average departure angle of the stream reach from a north-south (N-S) reference line when looking south. For streams oriented N-S, the azimuth is 0°; streams oriented NW-SE, the azimuth is less than 0°; and streams oriented NE-SW, the azimuth is greater than 0°. Therefore, all stream reach azimuth angles are bounded between -90° and +90°.

The east side of the stream is always on the left-hand side because the azimuth is always measured looking south for streams located in the north latitudes. Note that an E-W oriented stream dictates the east or left-hand side by whether the azimuth is a -90° (left-hand is the north side) or +90° (left-hand is the south side).

The topographic altitude angle (α_t) is the vertical angle from a level line at the streambank to the general top of the local terrian when looking 90° from the general stream reach azimuth. There are two altitude angles -- one for for the left-hand and one for the right-hand sides. The altitude is 0 for level plain topography; $\alpha_t > 0$ for hilly or canyon terrian. The altitudes for opposite sides of the stream are not necessarily identical. Sometimes streams tend to one side of a valley or may be flowing past a bluff line.

The height of vegetation (V_h) is the average maximum existing or proposed height of the overstory riparian vegetation above the water surface. If the height of vegetation changes dramatically -- e.g., due to a change in type of vegetation -- then sudividing the reach into smaller subreaches may be warranted.

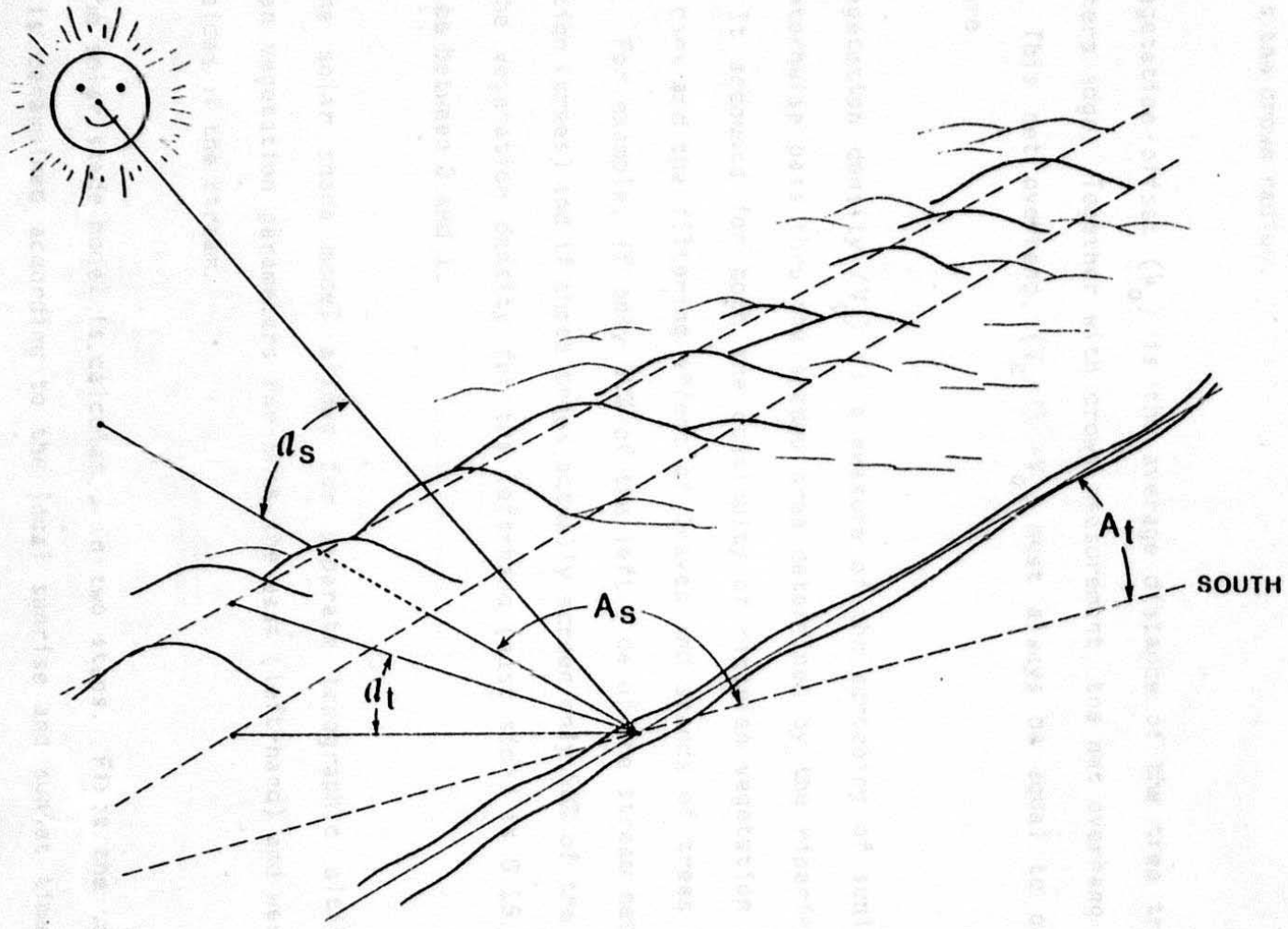

Figure 2.2. Local solar and stream orientation angular measurements.

Crown measurement (V_c) is a function of the crown diameter and accounts for overhang. Crown measurement for hardwoods is the crown diameter, softwoods is the crown radius.

Vegetation offset (V_o) is the average distance of the tree trunks from the waters edge. Together with crown measurement, the net overhang is determined. This net overhang, $(V_c/2) - V_o$, must always be equal to or greater than zero.

Vegetation density (V_d) is a measure of the screening of sunlight that would otherwise pass thru the shaded area determined by the riparian vegetation. It accounts for both the continuity of riparian vegetation along the stream bank and the filtering effect of leaves and stands of trees along the stream. For example, if only 50% of the left side of the stream has riparian vegetation (trees) and if those trees actually screen only 50% of the sunlight, then the vegetation density for the left-hand (east side) is 0.25. V_d must always be between 0 and 1.

The solar shade model allows for separate topographic altitudes and riparian vegetation parameters for both the east (left-hand) and west (right-hand) sides of the stream.

The solar shade model is calculated in two steps. First the topographic shade is determined according to the local sunrise and sunset times for the specified time of year. Then the riparian shade is calculated between the local sunrise and sunset times.

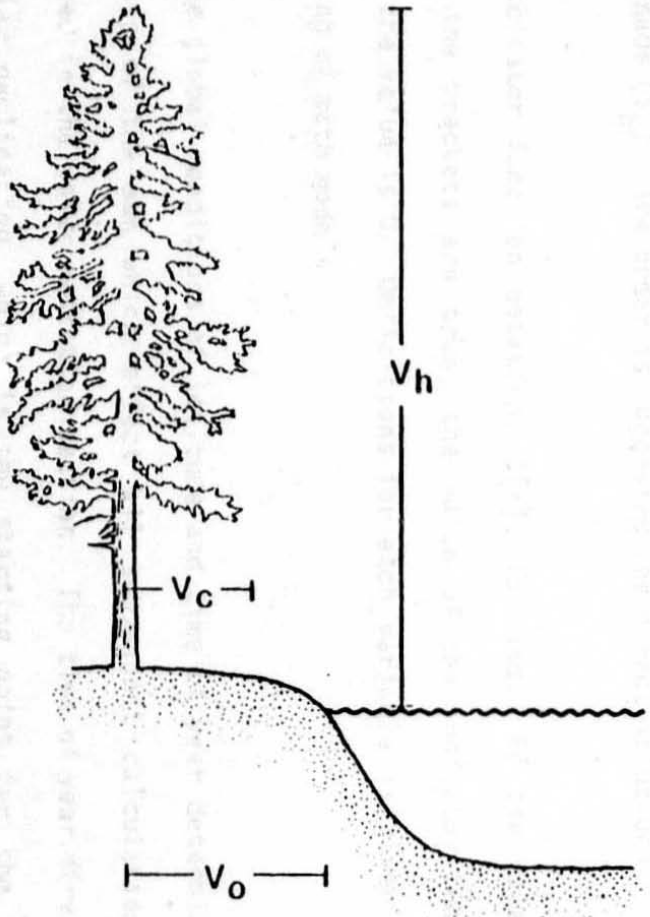

Vc ≡ diameter, hardwoods
≡ radius, softwoods

Vd ≡ ratio of shortwave radiation eliminated to incoming over entire reach shaded area

Figure 2.3. Riparian vegetation shade parameters.

Topographic shade is defined as the ratio of that portion of solar radiation excluded between level-plain and local sunrise/sunset to the solar radiation between level-plain sunrise and sunset.

Riparian vegetation shade is defined as the ratio for that portion of the solar radiation over the water surface intercepted by the vegetation between local sunrise and sunset to the solar radiation between level-plain sunrise and sunset.

The following math models are based upon the previous rationals. There are five groupings of these models: (1) level-plain sunrise/sunset hour angle and azimuth (h_s and A_{so}), (2) local sunrise/sunset altitude (α_{sr} and α_{ss}), (3) topographic shade (S_t), (4) riparian vegetation shade (S_v), and (5) total solar shade (S_h). The order is suggested for direct solutions.

Indicator function notation, $I[\bullet]$, is used. If the relationship shown within the brackets are true, the value of the indicator function is 1; if false, the value is 0. Definitions for each variable is given after the last groupting of math models.

The global conditions of latitude and time of year determine the relative movements of the sun which affect all subsequent calculations. They were explained in the solar radiation section. The time of year directly determines the solar declination, which is the starting point for the following math models.

LEVEL-PLAIN SUNRISE/SUNSET HOUR ANGLE AND AZIMUTH

The level-plain sunrise/sunset group of math models are to determine the hour angle and corresponding solar azimuth at sunrise and sunset. The solar movements are symetrical about solar noon; i.e., the absolute values of the sunrise and sunset parameters are identical, they differ only in sign. The math model is:

$$\delta = 0.40928 \cos[(2\pi/365)\ (172 - D_i)]$$

$$h_s = \arccos\ [-(\sin \phi \sin \delta)/(\cos \phi \cos \delta)]$$

$$A_{so} = \begin{cases} \arcsin\ (\cos \delta \sin h_s) & ;\delta \leq \phi \\ \pi - \arcsin\ (\cos \delta \sin h_s) & ;\delta > \phi \end{cases}$$

The level-plain sunrise hour angle is equal to $-h_s$; the sunset hour angle is h_s. The hour angles are referenced to solar noon ($h = 0$). Therefore, the duration from sunrise to solar noon is the same as from solar noon to sunset. One hour of time is equal to 15° of hour angle.

The solar azimuth at sunrise is $-A_{so}$; the sunset azimuth is A_{so}. Azimuths are referenced from the north-south line looking south for streams located in the north latitudes.

LOCAL SUNRISE/SUNSET ALTITUDES

Local sunrise and sunset is a function of the local topography as well as the global conditions. Furthermore, the local terrain may not be identical on opposite sides of the stream. Also, some streams are oriented such that the

sun may rise and set on the same side of the stream during part or even all of the year. The following local sunrise/sunset models properly account for the relative location of the sun with respect to each side of the stream.

The model for the local sunrise is:

$$\alpha_{tr} = \alpha_{te}\, I[-A_{so} \leq A_r] + \alpha_{tw}\, I[A_{so} > A_r]$$

$$h_{sr} = -\arccos \{[\sin \alpha_{sr} - (\sin \phi \sin \delta)]/[\cos \phi \cos \delta]\}$$

$$A_{sr} = -\arcsin [\cos \delta \sin h_{sr})/[\cos \alpha_{sr})]$$

$$\alpha_{sr} = \arctan [(\tan \alpha_{tr}) (\sin|A_{sr} - A_r|)]$$

but, $\sin \alpha_{sr} \leq (\sin \phi \sin \delta) + (\cos \phi \cos \delta)$

The model for the local sunset is:

$$\alpha_{ts} = \alpha_{te}\, I[A_{so} \leq A_r] + \alpha_{tw}\, I[A_{so} > A_r]$$

$$h_{ss} = \arccos \{[\sin \alpha_{ss} - (\sin \phi \sin \delta)]/[\cos \phi \cos \delta]\}$$

$$A_{ss} = \arcsin [\cos \delta \sin h_{ss})/[\cos \alpha_{ss})]$$

$$\alpha_{ss} = \arctan [(\tan \alpha_{ss}) (\sin|A_{ss} - A_r|)]$$

but, $\sin \alpha_{ss} \leq (\sin \phi \sin \delta) + (\cos \phi \cos \delta)$

The reason for the restriction on the $\sin \alpha_{sr}$ and $\sin \alpha_{ss}$ is that the sun never raises higher in the sky than indicated for that latitude and time of year regardless of the actual topographic altitude. For example, an E-W oriented stream in the middle latitudes could be flowing through a deep canyon which is casting continuous shade for a portion of the winter months.

TOPOGRAPHIC SHADE

Once the level-plain and local sunsrise and sunset times are known, the topographic shade can be computed directly in closed form. The definition for topographic shade leads to the following:

$$S_t = \left\{ \left[\int_{-h_s}^{h_s} \sin \alpha \, dh \right] - \left[\int_{h_{sr}}^{h_{ss}} \sin \alpha \, dh \right] \right\} \Big/ \left\{ \int_{-h_s}^{h_s} \sin \alpha \, dh \right\}$$

$$= 1 \left\{ \left[\int_{h_{sr}}^{h_{ss}} \sin \alpha \, dh \right] \Big/ \left[\int_{-h_s}^{h_s} \sin \alpha \, dh \right] \right\}$$

which can be integrated directly to

$$S_t = 1 - \left\{ \left[(h_{ss} - h_{sr}) (\sin \phi \sin \delta) \right] - \left[(\sin h_{ss} - \sin h_{sr}) \right.\right.$$

$$\left.\left. (\cos \phi \cos \delta) \right] \Big/ \left\{ 2 \left[(h_s \sin \phi \sin \delta) + (\sin h_s \cos \phi \cos \delta) \right] \right\}$$

RIPARIAN VEGETATION SHADE

The riparian vegetation shade requires keeping track of the shadows cast throughout the sunlight time because only that portion over the water surface is of interest. The model must account for sun side of the stream and the length of the shadow cast over the water. The model is:

$$V_c = V_{ce} \, I[A_s \leq A_r] + V_{dw} \, I[A_s > A_r]$$

$$V_d = V_{de}\, I[A_s \le A_r] + V_{dw}\, I[A_s > A_r]$$

$$V_h = V_{he}\, I[A_s \le A_r] + V_{hw}\, I[A_s > A_r]$$

$$V_o = V_{oe}\, I[A_s \le A_r] + V_{ow}\, I[A_s > A_r]$$

$$\alpha = \sin^{-1}\left[(\sin\phi \sin\delta) + (\cos\phi \cos\delta \cos h)\right]$$

$$A_s = \sin^{-1}\left[(\cos\delta \sin h) / (\cos\alpha)\right]$$

$$B_s = \left[(V_h \cot\alpha)\,(\sin/A_s - A_r/)\right] + \left[(V_c/2) - V_o\right]$$

but, $(V_c/2) - V_o \ge 0$

$$0 \le B_s \le \bar{B}$$

$$S_v = \left\{ \int_{h_{sr}}^{h_{ss}} (V_d\, B_s \sin\alpha)\,dh \right\} \Big/ \left\{ \int_{-h_s}^{h_s} (\bar{B} \sin\alpha)\,dh \right\}$$

It is not possible to integrate equation ____ completely, so a numerical integration method is required. The suggested numerical approximation is:

$$S_v = \left\{ \left[\sum_{h_{sr}}^{h_{ss}} (V_d\, B_s \sin\alpha) \right] \Delta h \right\} \Big/ \left\{ 2\bar{B} \left[(h_s \sin\phi \sin\delta) + (\sin h_s \cos\phi \cos\delta) \right] \right\}$$

Equations ____ through ____ are used to determine the jth value of V_d, B_s, and α for $h_j = h_{sr} + j\Delta h$. Sixteen intervals, or $\Delta h = (h_{ss} - h_{sr})/16$, will give better than 1% precision when using the trapezoidal rule and better than .01% precision when using Simpson's rule for functions without discontinuities.

However, the function will have a discontinuity if the stream becomes fully shaded due to riparian vegetation after sunrise or before sunset.

SOLAR SHADE FACTOR

The solar shade factor is simply the sum of the topographic and riparian vegetation shades. It is:

$$S_h = S_t + S_v$$

Since the solar declinition and subsequent solar related parameters depend upon the time of year, it will be necessary to calculate the various shade factors for each day of the time period to obtain the average factor for the time periods. This will result in shade factors completely compatible with the heat flux components. This is done by:

$$S_h = \left[\sum_{i=n}^{N} (S_{t,i} + S_{v,i}) \right] \Big/ \left[N-n+1 \right]$$

DEFINITIONS

The following definitions pertain to all the variables used in this solar shade section:

α ≡ solar altitude, radians

α_{sr} ≡ local sunrise solar altitude, radians

α_{ss} ≡ local sunset solar altitude, radians

α_{te} ≡ eastside topographic altitude, radians

α_{tr} ≡ sunrise side topographic altitude, radians

α_{ts} ≡ sunset side topographic altitude, radians

α_{tw} ≡ westside topographic altitude, radians

A_r ≡ stream reach azimuth, radians

A_s ≡ local azimuth at time h, radians

A_{so} ≡ level-plain sunset azimuth, radians

A_{sr} ≡ local sunrise solar azimuth, radians

A_{ss} ≡ local sunset solar azimuth, radians

$\bar{B}$ ≡ average stream width, meters

B_s ≡ stream solar shade width, meters

D_i ≡ time of year, Julian day

S_i ≡ solar declination, radians

h ≡ solar hour angle, radians

h_s ≡ level-plain hour sunset hour angle, radians

h_{sr} ≡ local sunrise hour angle, radians

h_{ss} ≡ local sunset hour angle, radians

i ≡ day counter, Julian days

n ≡ first day in time period, Julian days

N ≡ last day in time period, Julian days

ϕ ≡ stream reach latitude, radians

S_h ≡ total solar shade, decimal

S_t ≡ topodraphic shade, decimal

S_v ≡ riparian vegetation shade, decimal

V_c ≡ riparian vegetation crown factor, meters; crown diameter for hardwoods, crown radius for softwoods

V_{ce} ≡ eastside crown factor, meters

V_{cw} ≡ westside crown factor, meters

V_{d} ≡ riparian vegetation density factor, decimal

V_{de} ≡ eastside density, decimal

V_{dw} ≡ westside density, decimal

V_{h} ≡ riparian vegetation height above water surface, meters

V_{he} ≡ eastside height, meters

V_{hw} ≡ westside height, meters

V_{o} ≡ riparian vegetation waterline offset distance, meters

V_{oc} ≡ eastside offset, meters

V_{ow} ≡ westside offset, meters

METEOROLOGY

There are five meteorological parameters used in the instream water temperature model: (1) air temperature, (2) humidity, (3) sunshine ratio/cloud cover, (4) wind speed, and (5) atmospheric pressure. The first four are expected as input data for a specific elevation in the basin. The meteroology model assumes adiabatic conditions to transpose the air temperature and humidity vertically throughout the basin. Atmospheric pressure is calculated directly from reach elevations. Sunshine ratio/cloud cover and wind speed is assumed constant throughout the basin.

ADIABATIC CORRECTION MODEL

The atmospheric pressure for each reach can be computed with sufficient accuracy directly from the respective reach elevations. The formula is:

$$P = 1013[(288-0.0065Z)/288]^{5.256} \qquad (\ )$$

where: P ≡ atmospheric pressure at elevation Z, mb.

Z ≡ average reach elevation, m.

Air temperatures generally decrease 2°F for every 1000 ft. increase in elevation. Therefore, correcting for the meteric system, the following formula is used:

$$R_{h_z} = R_{h_\phi} \cdot 1.064^{(T_{a\phi} - T_{az})} \cdot \left[\frac{(288 - 0.0065\,z)/288}{(288 - 0.0065\,z_0)/288}\right]^{5.256}$$

$\frac{R_{h_z}}{R_{h\phi}}$ assume $z_0 = 0$ $\quad T_{az} = T_{a\phi} - 0.00656\,(z - z_0)$

& $T_{a\phi} = 20°C$

$$\frac{R_{h_z}}{R_{h\phi}} = 1.064^{(0.00656\,z)} \cdot \left(\frac{288 - 0.0065\,z}{288}\right)^{5.256}$$

June

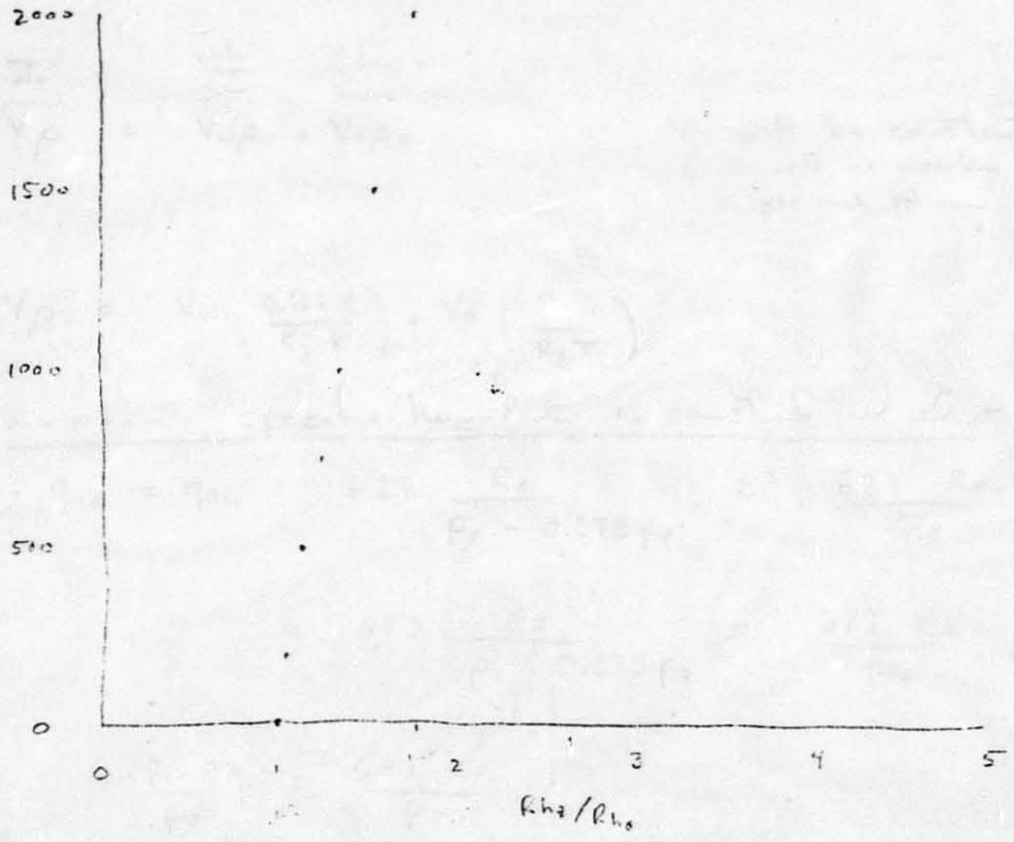

$e_{a_0} = Rh_0 \, e_s \qquad e_s = 6.60 \cdot 1.064^{T_{a_0}}$, Rh_0 given

$e_{a_z} = ?$

$$\rho_0 = \frac{P_0}{R_d T_0} \left(1 - 0.378 \frac{e_{a_0}}{P_0}\right)$$

$$\rho_z = \frac{P_z}{R_d T_z} \left(1 - 0.378 \frac{e_{a_z}}{P_z}\right)$$

moist air: $\rho_v = \rho_w + \rho_d$ (water vapor, dry air)

V will be constant (we will be working in per unit volume)

$$\rho_v = \rho_w \left(\frac{0.622\, e}{R_d T}\right) + \rho_d \left(\frac{P_d}{R_d T}\right)$$

can assume specific humidity is constant w/ elev

$$q_{h_0} = q_{h_z} = \frac{622\, e_0}{P_z - 0.378 P_0} \approx \frac{622\, e_0}{P_0}$$

$$= \frac{622\, e_z}{P_z - 0.378 P_z} \approx \frac{622\, e_z}{P_z}$$

$$\frac{622\, e_0}{P_0} = \frac{622\, e_z}{P_z}$$

$$e_z = \frac{e_0}{P_0} P_z = \frac{Rh_0 \, e_{s_0}}{P_0} P_z = Rh_z \, e_{s_z}$$

$$Rh_z = Rh_0 \, \frac{6.60 \cdot 1.064^{T_{a_0}}}{6.60 \cdot 1.064^{T_{a_z}}} \cdot \frac{P_z}{P_0}$$

$$Rh_z = Rh_0 \cdot 1.064^{(T_{a_0} - T_{a_z})} \cdot \frac{(288 - 0.0065 z_z / 288)^{5.256}}{(288 - 0.0065 z_0 / 288)^{5.256}}$$

Fredz Kh ...

$$\frac{Rh_z}{Rh_0} = \frac{1.064^{T_\phi}}{1.064^{T_z}} \cdot \frac{T_z + 273}{T_0 + 273}$$

$$\frac{e_{az}/e_{cz}}{e_{a0}/e_{c0}} = \frac{e_{c0}}{e_{cz}} \cdot \frac{T_z + 273}{T_0 + 273}$$

$$\frac{e_{az}\ e_{c\phi}}{e_{a0}\ e_{cz}} = \frac{e_{c\phi}}{e_{cz}} \frac{T_z + 273}{T_0 + 273}$$

$$R_{h_z} = R_{h_\phi} \cdot 1.064^{(T_{a_\phi} - T_{a_t})} \left[\frac{(288 - 0.0065\, z)/288}{(288 - 0.0065\, z_0)/288} \right]^{5.256}$$

for $z_0 = 105$ $\quad C_T = 0.00656$

$$T_{a_z} = T_{a_\phi} - 0.00656\,(z - 105)$$

$$\frac{288 - 0.0065\,(105)}{288} = 0.99762$$

$$R_{h_z} = R_{h_\phi} \cdot 1.064^{0.00656\,(z - 105)} \left[\frac{(288 - 0.0065\, z)/288}{0.99763} \right]^{5.256}$$

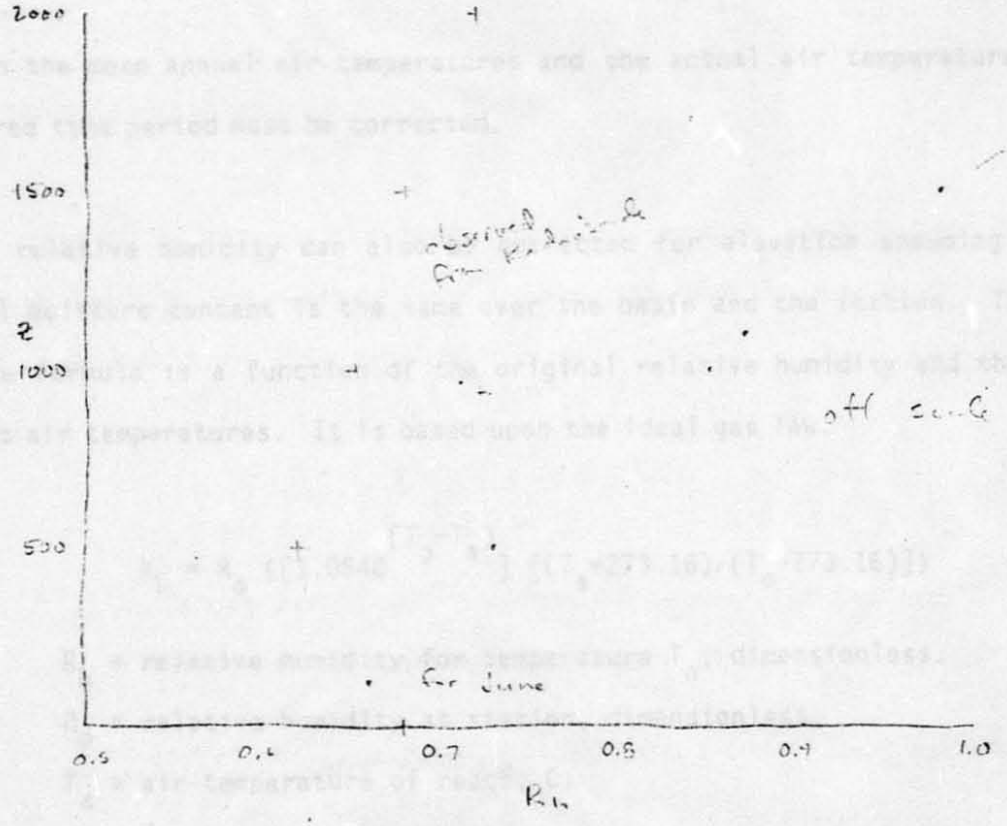

$$T_a = T_o - C_T (Z-Z_o) \qquad (\ )$$

where: $T_a \equiv$ air temperature at elevation E, C

$T_o \equiv$ air temperature at elevation E_o, C

$Z \equiv$ average elevation of reach, m

$Z_o \equiv$ elevation of station, m

$C_T \equiv$ adiabatic temperature correction coefficient = 0.00656 C/m

Both the mean annual air temperatures and the actual air temperature for the desired time period must be corrected.

The relative humidity can also be corrected for elevation assuming that the total moisture content is the same over the basin and the station. Therefore, the formula is a function of the original relative humidity and the two different air temperatures. It is based upon the ideal gas law.

$$R_h = R_o \{[1.0640^{(T_o-T_a)}] [(T_a+273.16)/(T_o+273.16)]\} \qquad (\ )$$

where: $R_h \equiv$ relative humidity for temperature T_a, dimensionless.

$R_o \equiv$ relative humidity at station, dimensionless.

$T_a \equiv$ air temperature of reach, C.

$T_o \equiv$ air temperature at station, C.

$0 \leq R_h \leq 1.0$

The sunshine factor is assumed to be the same over the entire basin as over the station. There is no known way to correct the windspeed for transfer to the basin. Certainly local topographic features will influence the wind-

speed over the water. However, the station windspeed is, at least, an indicator of the basin windspeed. Since the windspeed affects only the convection and evaporation heat flux components and these components have the least reliable coefficients in these models, the windspeed can be used as an important calibration parameter when actual water temperature data is available.

AVERAGE AFTERNOON METEOROLOGICAL CONDITIONS

The average afternoon air temperature is greater than the daily air temperature because the maximum air temperature usually occurs during the middle of the afternoon. This model assumes that

$$\bar{T}_{ax} = [(5T_{ax}) + (11\bar{T}_a)]/16 \qquad (\ )$$

where: $\bar{T}_{ax}$ ≡ average daytime air temperature between noon/sunset, C.

T_{ax} ≡ maximum air temperature during the 24-hour period, C.

$\bar{T}_a$ ≡ average daily air temperature during the 24-hour period, C.

A regression model was selected to incorporate the significant daily meteorological parameters to estimate the incremental increase of the average daytime air temperature above the daily. The resulting average daytime air temperature model is

$$\bar{T}_{ax} = T_a + [a_o + a_1 H_{sx} + a_2 R_h + a_3 (S/S_o)] \qquad (\ )$$

where: T_{ax} ≡ maximum air temperature, C.

$\bar{T}_a$ ≡ daily air temperature, C.

H_{sx} ≡ extra-terresterial solar radiation, J/m²/sec.

R_h ≡ relative humidity, decimal.

S/S_o ≡ percent possible sunshine, decimal.

a_o thru a_3 ≡ regression coefficients.

Some regression coefficients were determined for the "normal" meteorological conditions at 16 selected weather stations. These coefficients and their respective coefficient of multiple correlations R, standard deviation of maximum air temperatures $S.T_{ax}$, and probable differences δ are given in Table B1.

The corresponding afternoon average relative humidity is

$$R_{hx} = R_h \, [1.0640^{(\bar{T}_a - \bar{T}_{ax})}][(\bar{T}_{ax}+273.16)/(\bar{T}_a+273.16)] \qquad (\ )$$

where: R_{hx} ≡ average afternoon relative humidity, dimensionless.

R_h ≡ average daily relative humidity, dimensionless.

$\bar{T}_a$ ≡ daily air temperature, C.

$\bar{T}_{ax}$ ≡ average afternoon air temperature, C.

Table B1

Station name	$\bar{R}$	$C_{S.T_{ax}}$	C_{δ}	Regression coefficients a_o	a_1	a_2	a_3
Phoenix, AZ	.936	0.737	0.194	11.21	-.00581	- 9.55	3.72
Santa Maria, CA	.916	0.813	0.243	18.90	-.00334	-18.85	3.18
Grand Junction, CO	.987	0.965	0.170	3.82	-.00147	- 2.70	5.57
Washington, DC	.763	0.455	0.219	6.64	-.00109	- 7.72	4.85
Miami, FL	.934	0.526	0.140	29.13	-.00626	-24.23	-7.45
Dodge City, KA	.888	0.313	0.107	7.25	-.00115	- 5.24	4.40
Caribou, ME	.903	0.708	0.226	0.87	.00313	0.09	7.86
Columbia, MO	.616	0.486	0.286	4.95	-.00163	- 2.49	4.54
Great Falls, MT	.963	1.220	0.244	9.89	.00274	- 9.56	1.71
Omaha (North), NE	.857	0.487	0.187	9.62	-.00279	- 9.49	6.32
Bismark, ND	.918	1.120	0.332	11.39	-.00052	-13.03	5.97
Charleston, SC	.934	0.637	0.170	9.06	-.00325	- 8.79	7.42
Nashville, TN	.963	0.581	0.117	5.12	-.00418	- 4.55	9.47
Brownsville, TX	.968	0.263	0.049	9.34	-.00443	- 4.28	0.72
Seattle, WA	.985	1.180	0.153	-9.16	.00824	12.79	3.86
Madison, WI	.954	0.650	0.145	1.11	.00219	1.80	3.96
ALL	.867	1.276	0.431	6.64	-.00088	- 5.27	4.86

HEAT FLUX

THERMAL PROCESSES

There are five basic thermal processes recognized by the heat flux relationships: (1) radiation, (2) evaporation, (3) convection, (4) conduction, and (5) the conversion from other energy forms to heat.

THERMAL SOURCES

The various relationships for the individual heat fluxes will be discussed here. Each is considered mutually exclusive and when added together account for the heat budget for a single column of water. A heat budget analysis would be applicable for a stationary tank of continuously mixed body of water. However, the transport model is necessary to account for the spatial location of the column of water at any point in time.

RADIATION

Radiation is an electomagnetic mechanism, which allows energy to be transported at the speed of light through regions of space that are devoid of matter. The physical phenomena causing radiation is sufficiently well-understood to provide very dependable source-component models. Radiation models have been theoretically derived from both thermodynamics and quantum

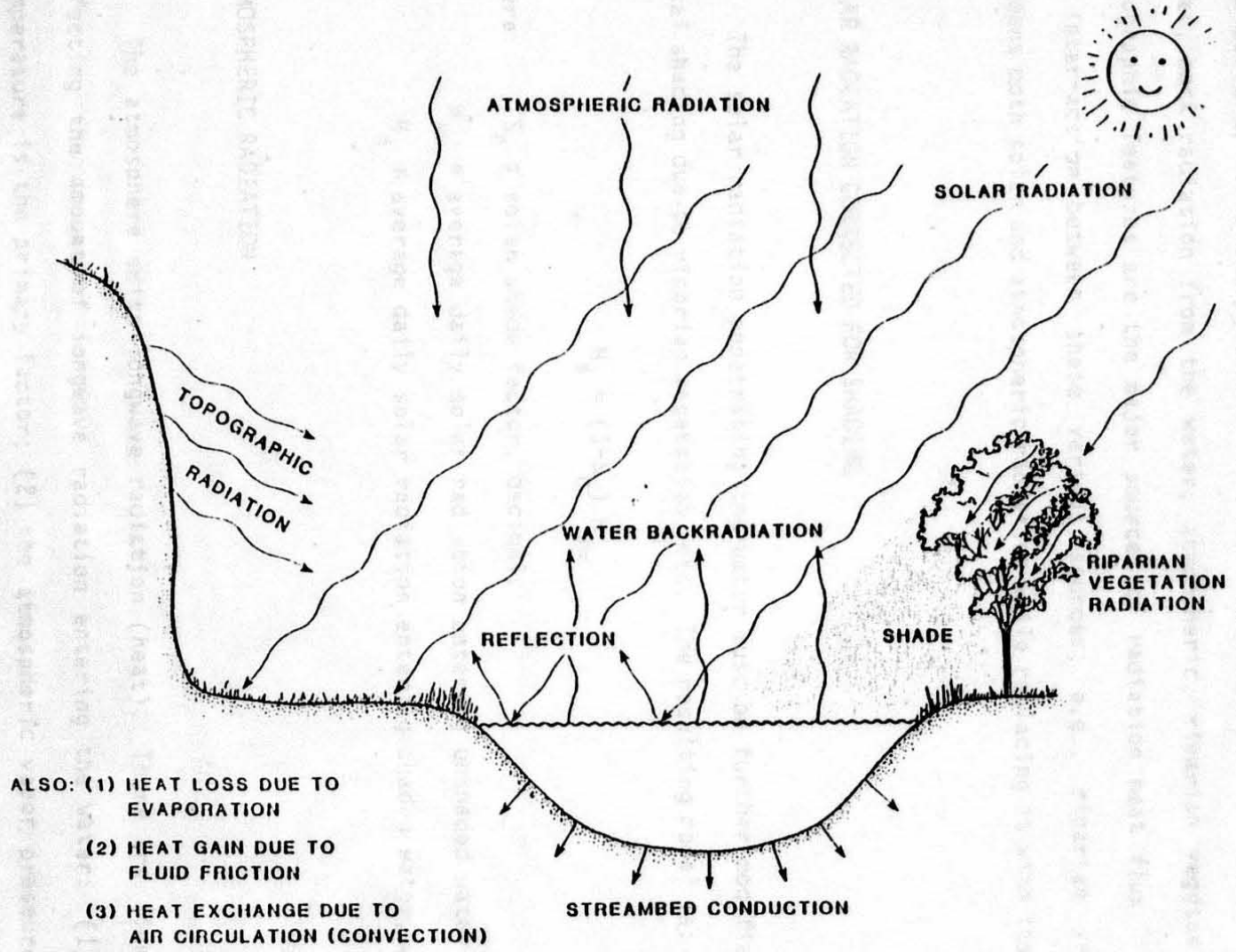

Figure 2.4. Heat flux sources.

physics and have been experimentally verified with a high degree of precision and reliability. It provides the most dependable components of the heat flux submodel and, fortunately, is also the most important source of heat exchange. Solar, back radiation from the water, atmospheric, riparian vegetation, and topographic features are the major sources of radiation heat flux. There is an inter-action between these various sources; e.g., riparian vegetation screens both solar and atmospheric radiation while replacing it with its own.

SOLAR RADIATION CORRECTED FOR SHADING

The solar radiation penetrating the water must be further modified by the local shading due to riparian vegetation, etc. The resulting model is:

$$H_s = (1-S_h)\, H_{sw} \qquad (\ )$$

where: $S_h \equiv$ solar shade factor, decimal.

$H_{sw} \equiv$ average daily solar radiation entering unshaded water, $J/m^2/sec.$

$H_s \equiv$ average daily solar radiation entering shaded water, $J/m^2/sec.$

ATMOSPHERIC RADIATION

The atmosphere emits longwave radiation (heat). There are five factors affecting the amount of longwave radiation entering the water: (1) the air temperature is the primary factor; (2) the atmospheric vapor pressure affects the emissivity; (3) the cloud cover converts the shortwave solar radiation

into additional longwave radiation, sort of "hot spots" in the atmosphere; (4) the reflection of longwave radiation at the water-air interface; and (5) the interception of longwave radiation by vegetative canopy cover or shading. An equation which approximates longwave atmospheric radiation entering the water is:

$$H_a = (1-r_\ell)(1-S_a)(1+kC_\ell^2)\ [\varepsilon_a \sigma (T_a+273.16)^4] \qquad (\ )$$

where: $C_\ell = [1-(S/S_o)]^{3/5}$ ≡ cloud cover, decimal

S/S_o ≡ sunshine ratio, decimal

k ≡ type of cloud cover factor, $0.04 \le k \le 0.24$

ε_a ≡ atmospheric emissivity, decimal

S_a ≡ atmospheric shade factor, decimal

r_ℓ ≡ longwave radiation reflection, decimal

T_a ≡ air temperature, C

$\sigma = 5.672 \cdot 10^{-8}$, $J/m^2/sec/K^4$ ≡ Stefen-Boltzman constant.

The preferred estimate of ε_a is:

$$\varepsilon_a = a+b\sqrt{e_a}, \text{ decimal}$$

$$a = 0.61$$

$$b = 0.05$$

e_a ≡ vapor pressure = $R_h\ [6.60(1.0640)^{T_a}]$, mb

CLOUD, HUMID, TAIR,

CLOUD = (1 - SUN)**

HUMID = HUMIDØ • (1.064 - DT) • (1 - DT / (TAIRØ + 273.16))

TAIR = TAIRØ - DT

DT = 0.00656 • (ELEV - ELEVØ) = 0

HUMID = 0.712

TAIR = 31.9

An alternate estimate of ε_a is:

$$\varepsilon_a = 9.062 \cdot 10^{-6} (T_a + 273.16)^2, \text{ decimal}$$

The preferred estimate accounts for water vapor which also absorbs solar radiation which, in turn, is converted into longwave radiation. If the absorbtion of solar is overpredicted, then some of the overprediction is returned as longwave and vice versa. Therefore, errors in one (solar) tend to be compensated by the other (atmospheric). The alternate form is mentioned in the literature as a simpler model and possibly a better predictor of longwave radiation alone. However, for purpose of predicting water temperatures, it ultimately makes little difference as to the form of radiation (short or longwave) as long as the total heat exchange is accurately predicted. The alternate form is only used when the solution technique requires simple steps.

Assuming $k = 0.17$, $r_\ell = 0.03$, and using the preferred estimate of ε_a, this equation reduces to:

$$H_a = (1-S_a)(1+0.17C_\ell^2)[3.36+0.706(R_h \cdot 1.0640^{T_a})^{1/2}][10^{-8}(T_a+273.16)^4] \quad (\ )$$

The atmospheric shade factor (S_a) is assumed to be identical to the solar shade factor (S_h).

TOPOGRAPHIC FEATURES RADIATION

Currently, the radiation from topographic features is assumed to be included as a part of the riparian vegetation radiation. Therefore, no separate component model is used.

RIPARIAN VEGETATION RADIATION

The riparian vegetation intercepts all other forms of radiation and radiates its own. Essentially it totally eliminates the estimated shade amount of solar, but replaces the other longwave sources with its own longwave source. The difference is mostly in the emissivity between the different longwave sources. The model is:

$$H_v = (\varepsilon_v \sigma)\ S_v\ (T_a + 273.16)^4 \qquad (\ )$$

where: $\varepsilon_v \equiv$ vegetation emissivity = 0.9526 decimal

$\sigma \equiv$ Stefan-Boltzman constant = $5.672 \cdot 10^{-8}$ J/m²/sec/K⁴

$H_v \equiv$ riparian vegetation radiation, J/m²sec

$S_v \equiv$ riparian vegetation shade factor, decimal

$T_a \equiv$ riparian vegetation temperature, assumed to be the ambient air temperature, C

The riparian vegetation shade factor (S_v) is assumed to be identical to the solar shade factor (S_h).

WATER RADIATION

The water emits radiation and this is the major balancing heat flux which prevents the water temperature from increasing without bounds. The model is:

$$\hat{H}_w = \varepsilon_w \sigma (T_w + 273.16)^4 \qquad (\ )$$

where: $\hat{H}_w \equiv$ water radiation, $J/m^2/sec$

$T_w \equiv$ water temperature, C

$\varepsilon_w \equiv$ water emissivity = 0.9526 decimal

$\sigma \equiv$ Stefan-Boltzman constant = $5.672 \cdot 10^{-8}$ $J/m^2/sec/K^4$

A first-order approximation to equation A36 with less than ± 1.8% error of predicted radiation for $0C \leq T_w \leq 40C$ is:

$$\hat{H}_w = 300 + 5.500\ T_w \qquad (\ )$$

where: $\hat{H}_w \equiv$ approximate water radiation, $J/m^2/sec$

$T_w \equiv$ water temperature, C

STREAM EVAPORATION

Evaporation, and its counterpart condensation, requires an exchange of heat. The isothermal (same temperature) conversion of liquid water to vapor requires a known fixed amount of heat energy called the heat of vaporization. Conversely, condensation releases the same amount of heat. The rate of evaporation -- the amount of liquid water converted to vapor -- is a function of both

the circulation and vapor pressure (relative humidity) of the surrounding air. If the surrounding air were at 100% relative humidity, no evaporation would occur. If there were no circulation of air, then the air immediately above the water surface would quickly become saturated and no further net evaporation would occur.

Evaporation, while second in importance to radiation, is a significant form of heat exchange. Most available models are derived from lake environments and are probably the least reliable of the thermal processes modeled. However, one model was derived from a single set of open channel flow data. Both model types are offered. They differ only in the wind function used. The wind function for the flow-type model was adjusted by approximately 3/4 to better match recorded field data.

Two evaporation models are available. They differ only in the wind function assumed. The first is the simplest. It was obtained largely from lake data, and is used only for small hand held calculator solutions techniques. The second is the preferred. It was obtained from open channel flow data, and is used for all but the simplest solutions technique.

The lake-type model is:

$$H_e = (26.0W_a)[R_h(1.0640)^{T_a} - (1.0640)^{T_w}] \qquad (\ )$$

The flow-type model is:

$$H_e = (40.0 + 15.0W_a)[R_h(1.0640)^{T_a} - (1.0640)^{T_w}] \quad (\ )$$

where: $H_e \equiv$ evaporation heat flux, J/m²/sec

$W_a \equiv$ wind speed, m/sec

$R_h \equiv$ relative humidity, decimal

$T_a \equiv$ air temperature, C

$T_W \equiv$ water temperature, C

CONVECTION

Convection can be an important source of heat exchange at the air-water interface. Air is a poor conductor, but the ability of the surrounding air to circulate, either under forced conditions from winds or freely due to temperature differences, constantly exchanges the air at the air-water interface. Convection affects the rate of evaporation and, therefore, the models are related. But the actual heat exchange due to the two different sources are mutually exclusive. Convection is not quite as important as evaporation as a source of heat flux but is still significant. The available models suffer from the same defects since both use the same circulation model.

The heat exchange at the air-water interface is due mainly to convection of the air. Air is a poor conductor, but the ability of the atmosphere to convect freely constantly exchanges the air at the air-water interface. The current models are largely based upon lake models but will be used here. The

convection model is based upon the evaporation model using what is called the Bowen ratio; i.e.

$$\text{Bowen ratio} = B_f\, P(T_w - T_a)/(e_s - e_a) \qquad (\ )$$

where:

P ≡ atmospheric pressure, mb

T_w ≡ water temperature, C

T_a ≡ air temperature, C

e_s ≡ saturation vapor pressure, mb

e_a ≡ air vapor pressure, mb

B_f ≡ Bowen ratio factor

Air convection heat exchange is approximated by the product of the Bowen ratio and the evaporation heat exchange:

$$H_c = RH_e \qquad (\ )$$

where:

H_c ≡ air convection heat flux, $J/m^2/sec$

R ≡ Bowen ratio, decimal

H_e ≡ evaporated heat flux, $J/m^2/sec$

Since the air convection heat flux is a function of the evaporation heat flux, two models are offered. The first, the simplest, is a lake-type model. The second, the preferred, is a flow-type model.

The lake-type model is:

$$H_c = (2.55 \cdot 10^{-3} W_a)\, P(T_w - T_a) \qquad (\ )$$

The flow-type model is:

$$H_c = (3.75 \cdot 10^{-3} + 1.40 \cdot 10^{-3} W_a)\, P(T_w - T_a) \qquad (\ )$$

where: $H_c \equiv$ air convection heat flux, J/m²/sec

$W_a \equiv$ wind speed, m/sec

$P \equiv$ atmospheric pressure, mb

$T_w \equiv$ water temperature, C

$T_a \equiv$ air temperature, C

STREAMBED CONDUCTION

Conduction occurs when a temperature gradient -- a temperature difference between two points -- exists in a material medium in which there is molecular contact. The only important conduction heat flux component is through the streambed. The thermal processes are reasonably well-understood although some of the necessary data may not be easily obtained without certain assumptions. However, the importance of this component, while not negilible, does allow for some liberties and suitable predictions can be made for most applications.

Streambed conduction is a function of the difference in temperature of the streambed at the water-streambed interface and the streambed at an equilibrium ground temperature at some depth below the streambed elevation, this equilibrium depth, and the thermal conductivity of the streambed material. The equation is:

$$H_d = K_g[(T_g - T_w)/\Delta Z_g] \qquad (\ )$$

where: H_d = conduction heat flux, J/m²/sec

K_g ≡ thermal conductivity of the streambed material, J/m/sec/C

T_g ≡ streambed equilibrium temperature, C

T_w ≡ streambed temperature at the water-streambed interface, assumed to to be the water temperature, C

ΔZ_g ≡ equilibrium depth from the water-streambed interface, m

K_g = 1.65 J/m/sec/C for water-saturated sands and gravel mixtures (Plukowski, 1970)

STREAM FRICTION

Heat is generated by fluid friction, either as work done on the boundaries or as internal fluid shear, as the water flows downstream. That portion of the potential energy (elevation) of the flowing water that is not converted to other uses (e.g., hydroelectric generation) is converted to heat. When ambient conditions are below freezing and the water in a stream is still flowing, part of the reason may be due to this generation of heat due to friction. The available model is straight-forward, simple to use, and solidly justified by basic physics. However, fluid friction is the least significant source of heat flux, but it can be noticeable for steep mountain streams.

The stream friction model is:

$$H_f = 9805\ (Q/\bar{B})S_f \qquad (\ )$$

where: H_f ≡ fluid friction heat flux, J/m²/sec

S_f ≡ rate of heat energy conversion, generally the stream gradient, m/m.

$Q \equiv$ discharge, cms.

$\bar{B} \equiv$ average top width, m

NET HEAT FLUX

The various heat flux components, when added together, form the net heat flux equation, i.e.,

$$H_n = H_a + H_c + H_d + H_e + H_s + H_v - H_w \qquad (\ )$$

where: H_a, etc. are as previously defined

$H_n \equiv$ net heat flux

When the equations for the separate components are substituted into equation D1, it can be reduced to:

$$H_n = A(T_w+273.16)^4 + BT_w + C\,(1.0640)^{T_w} - D \qquad (\ )$$

where: $A = 5.40 \cdot 10^{-8}$

$B = (C_r \cdot C_e\, P) + (K_g/\Delta Z g)$

$C = (40.0 + 15.0W_a)$

$D = H_a + H_f + H_s + H_v + (C_r \cdot C_e\, PT_a) +$

$[T_g(K_g/\Delta Z_g)] + [C_e\, R_h\, (1.0640^{T_a})]$

$C_e = a + bW_a + c\sqrt{W_a}$

$C_r = B_f/6.60$

The equilibrium water temperature T_e is defined to be the water temperature when the net heat flux is zero for a constant set of input parameters; i.e.,

$$A(T_e+273.16)^4 + BT_e + C\,(1.0640)^{T_e} - D = 0 \qquad (\ )$$

where: A, B, C, and D are as defined above.

The solution of equation D3 for T_e, given A, B, C, and D, is the equilibrium water temperature of the stream for a fixed set of meterologic, hydrologic, and stream geometry conditions. A physical analology is that as a constant discharge of water flows downstream in a prismatic stream reach under a constant set of meterologic conditions, then the water temperature will asymptotically approach the equilibrium water temperature regardless of the initial water temperature.

The first order thermal exchange coefficient K_1 is the first derivative of equation D2 taken at T_e.

$$K_1 = 4A(T_e+273.16)^3 + B + [C\ln(1.0640)]\,(1.0640)^{T_e} \qquad (\ )$$

where: T_e, A, B, and C are as defined above.

The second order thermal exchange coefficient is the coefficient for a second order term that collocates the actual heat flux at the initial water temperature (T_o) with a first-order Taylor series expansion about T_e.

$$K_2 = \{[A(T_o+273.16)^4 + BT_o + C(1.0640)^{T_o} - D]-[K_1(T_o-T_e)]\}/[(T_o-T_e)^2] \qquad (\ )$$

where: A, B, C, D, K_1, T_o, and T_e are as defined before.

Therefore, a first-order approximation of equation D2 with respect to the equilibrium temperature is

$$H_n = K_1 (T_e - T_w) \qquad ( )$$

And a second order approximation of equation D2 with respect to the equilibrium temperature is

$$H_n = K_1 (T_e - T_w) + K_2 (T_e - T_w)^2 \qquad ( )$$

HEAT TRANSPORT

The heat transport model is based upon the dynamic temperature - steady flow equation. This equation, when expressed as an ordinary differential equation, is identical in form to the less general steady-state equation. However, it is different in how the input data is defined and in that the dynamic equation requires tracking the mass movement of water downstream. The simultaneous use of the two identical equations with different sets of input is acceptable since the actual water temperature passes through the average daily water temperature twice each day -- once at night and then again during the day. The steady-state equation assumes that the input parameters are constant for each 24-hour period. Therefore, the solar radiation, meterological, and hydrology parameters are 24-hour averages. It follows, then, that the predicted water temperatures are also 24-hour averages. Hence, the term "average daily" means 24-hour averages -- from midnight to midnight for each parameter.

The dynamic model allows the 24-hour period to be divided into night and day times. While the solar radiation and meterological parameters are different between night and day, they are still considered constant during the cooler nighttime period and different, but still constant, during the warmer daytime period. Since it is a steady flow model, the discharges are constant over the 24-hour period.

It can be visualized that the water temperature would be at a minimum at sunrise, continually rise during the day so that the average daily water

temperature would occur near noon and be maximum at sunset, and begin to cool so that average daily would again occur near midnight and return to a minimum just before sunrise where the cycle would repeat itself.

The steady-state equation, with input based upon 24-hour averages, can be used to predict the average daily water temperatures throughout the entire stream system network. Since these average daily values actually occur near mid-night and mid-day, the dynamic model can be used to track the column of water between mid-night and sunrise and between noon and sunset to determine the minimum nighttime and maximum daytime water temperature respectively. Of course, the proper solar radiation and meterological parameters reflecting night and daytime conditions must be used for the dynamic model.

The minimum/maximum simulation requires that the upstream average daily water temperature stations at mid-night/mid-day for the respective sunrise/ sunset stations be simulated. This step is a simple hydraulic procedure requiring only a means to estimate the average flow depth.

DYNAMIC TEMPERATURE - STEADY FLOW

A control volume for the dynamic temperature - steady flow equation is shown in Figure A1. It allows for lateral flow. To satisfy the fundamental laws of physics regarding conservation of mass and energy, the heat energy in the incoming waters less the heat energy in the outgoing water plus the net heat flux across the control volume boundaries must equal the change in heat

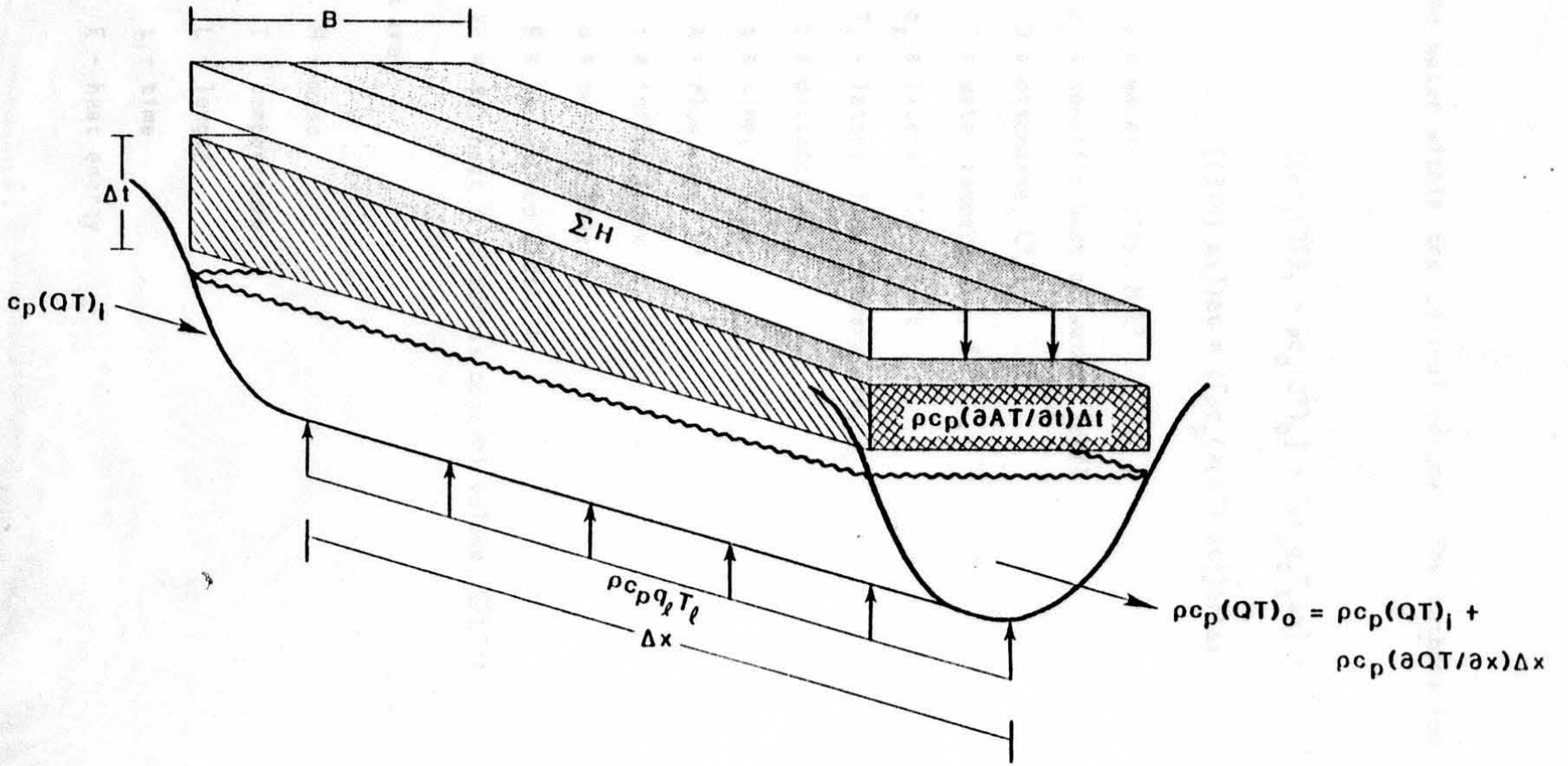

Figure 2.5. Dynamic energy control volume.

energy of the water within the control volume. The mathematical expression is:

$$\{[\rho c_p (QT)_i - \rho c_p (QT)_o] + [\rho c_p q_\ell T_\ell \Delta x] + [(B\Sigma H)\,\Delta x]\}\Delta t = \{[\rho c_p (\partial(AT)/\partial t)]\Delta t\}\Delta x \qquad (\ )$$

where:

ρ ≡ water density, M/L^3

c_p ≡ specific heat of water, $E/M/T$

Q ≡ discharge, L^3/t

T ≡ water temperature, T

q_ℓ ≡ lateral flow, L^2/t

T_ℓ ≡ lateral flow temperature, T

x ≡ distance, L

t ≡ time, t

A ≡ flow area, L^2

i ≡ inflow index

o ≡ outflow index

B ≡ stream top width, L

ΣH = net heat flux across control volume, $E/L^2/t$

note: units are

M - mass

T - temperature

L - length

t - time

E - heat energy

Equation A38 reduces to:

$$\partial(AT)/\partial t + \partial(QT)/\partial x = q_\ell T_\ell + (B\Sigma H)/(\rho c_p) \qquad (\ )$$

Assuming steady flow ($\partial A/\partial t=0$), letting $H_n = B\Sigma H$, recognizing $q_\ell \equiv \partial Q/\partial x$, and dividing through by Q, leads to:

$$(A/Q)\ (\partial T/\partial t) + \partial T/\partial x = (q_\ell/Q)\ (T_\ell - T) + H_n/(Q\rho c_p) \qquad (\ )$$

dynamic term

steady-state equation

dynamic temperature - steady flow equation

If the dynamic temperature term is neglected ($\partial T/\partial t = 0$), then the steady-state equation is left. Since the steady-state equation contains only a single independent variable x, it converts directly into an ordinary differential equation with no mathematical restrictions:

$$dT/dx = [(q_\ell/Q)\ (T_\ell - T)] + [H_n/(Q\rho c_p)] \qquad (\ )$$

If the dynamic temperature term is not neglected ($\partial T/\partial t \neq 0$), then equation A40 can still be solved using the classical mathematical technique known as the "Method of Characteristics". If, for notional purposes only, we substitute

$$\Phi \equiv (q_\ell/Q)\ (T_\ell - T) + H_n/(Q\rho c_p) \qquad (\ )$$

into equation A40 and use the definition of the total derivative for the dependent variable T, a resulting pair of dependent simultaneous first-order partial differential equations emerge

$$(A/Q)\ (\partial T/\partial t) + (1)\ (\partial T/\partial x) = \Phi \qquad (\ )$$

$$(dt)\ (\partial T/\partial t) + (dx)\ (\partial T/\partial x) = dT \qquad (\ )$$

Since the equations are dependent, the solution of the coefficient matrix is zero; i.e.,

$$\begin{bmatrix} (A/Q) & 1 \\ dt & dx \end{bmatrix} = 0$$

which leads to the characteristic line equation,

$$dx = (Q/A)dt \qquad (\ )$$

For the same reason, the solution matrix is also zero; i.e.,

$$\begin{bmatrix} \Phi & 1 \\ dt & dx \end{bmatrix} = 0$$

which leads to the characteristic integral equation,

$$dT/dx = [(q_\ell/Q)\ (T_\ell - T)] + [H_n/(Q\rho c_p)] \qquad (\ )$$

when Φ is replaced by its original terms of equation A42.

Equation A46 is identical in form to equation A41, and is valid for dynamic temperature conditions when solved along the characteristic line equation (equation A45). This presents no special problem since equation A45 simply tracts a column of water downstream -- an easily simulated task.

Closed-form solutions for the ordinary differential equation forms (equations A41 and A46) of the dynamic temperature-steady flow equations are possible with two important assumptions: (1) uniform flow exists, and (2) first and/or second order approximations of the heat flux versus water temperature relationships are valid.

FIRST-ORDER SOLUTIONS

First-order solutions are possible for all three cases of q_ℓ: Case 1, $q_\ell>0$; Case 2, $q_\ell<0$; and Case 3, $q_\ell=0$.

Case 1, $q_\ell>0$:

The ordinary differential equation with the first-order substitution is:

$$dT/dx = [(q_\ell/Q)\ (T_\ell - T)] + [K_1\ (T_e - T)\bar{B}/(\rho c_p Q)] \qquad (\ )$$

Since $Q = Q_o + q_\ell\ x$, equation D8 becomes

$$[Q_o + q_\ell x]\ dT/dx = \{[q_\ell T_\ell] + [(K_1\bar{B})/(\rho c_p)]T_e\} - \{q_\ell + [(K_1 W)/(\rho c_p)]\}T \qquad (\ )$$

let, $\quad a = [q_\ell T_\ell] + [(K_1\bar{B})/(\rho c_p)]T_e$

$\quad\ b = q_\ell + [(K_1\bar{B})/(\rho c_p)]$

Then D9 becomes

$$(Q_o + q_\ell x)\, dT/dx = a - bT \qquad (\ )$$

Using separation of variables,

$$\int_{T_o}^{T_w} \frac{dT'}{a-bT} = \int_0^{x_o} \frac{dx}{Q_o + q_\ell x} \qquad (\ )$$

and the solution is

$$T_w = (a/b) - [(a/b) - T_o]\,[1 + (q_\ell x_o/Q_o)]^{(-b/q_\ell)} \qquad (\ )$$

Case 2, $q_\ell < 0$:

If $q_\ell < 0$, then $T_\ell = T$ and equation D8 becomes

$$[Q_o + q_\ell x_o]\, dT/dx = [(K_1\bar{B})/(\rho c_p)]T \qquad (\ )$$

The solution is

$$T_w = T_e - [T_e - T_o]\,[1 + (q_\ell x_o/Q_o)]^{[(q_\ell - b)/q_\ell]} \qquad (\ )$$

Case 3, $q_\ell = 0$:

If $q_\ell = 0$, then $Q \neq Q(x)$ and equation D8 becomes

$$dT/dx = [(K_1\bar{B})/(\rho c_p Q)]T \qquad (\ )$$

The solution is

$$T_w = T_e - [T_e - T_o] \exp [-(K_1\bar{B}x_o)/(\rho c_p Q)] \qquad (\ )$$

SECOND-ORDER SOLUTIONS

A second-order solution for case 3 is as follows.

Let $q_\ell = 0$ and using equation A48 results in

$$dT/dx = [K_1(T_e - T) + K_2 (T_e - T)^2]\bar{B}/(\rho c_p Q) \qquad (\ )$$

The solution is

$$T_w = T_e - \frac{(T_e - T_o) \exp [- (K_1\bar{B}x_o)/(\rho c_p Q)]}{1 + (K_2/K_1) (T_e - T_o) \{1-\exp [-(K_1\bar{B}x_o)/(\rho c_p Q)]\}} \qquad (\ )$$

Using the first-order solution and making second-order corrections according to the form suggested by equation D18 results in

$$T_w = T_e' - [(T_e' - T_o) R]/[1 + (K_2/K_1) (T_e' - T_o) (1-R)] \qquad (\ )$$

where: $a = [q_\ell T_\ell] + [(K_1 B)/(\rho c_p)]T_e$

$b = q_\ell + (K_1 \bar{B})/(\rho c_p)$

Case 1. $q>0$:

$$T_e' = a/b$$

$$R = [1 + (q_\ell x_o/Q_o)]^{(-b/q_\ell)}$$

Case 2. $q<0$:

$$T_e' = T_e$$

$$R = [1 + (q_\ell x_o/Q_o)]^{[(q_\ell - b)/q_\ell]}$$

Case 3. $q=0$:

$$T_e' = T_e$$

$$R = \exp [-(bx_o)/Q_o]$$

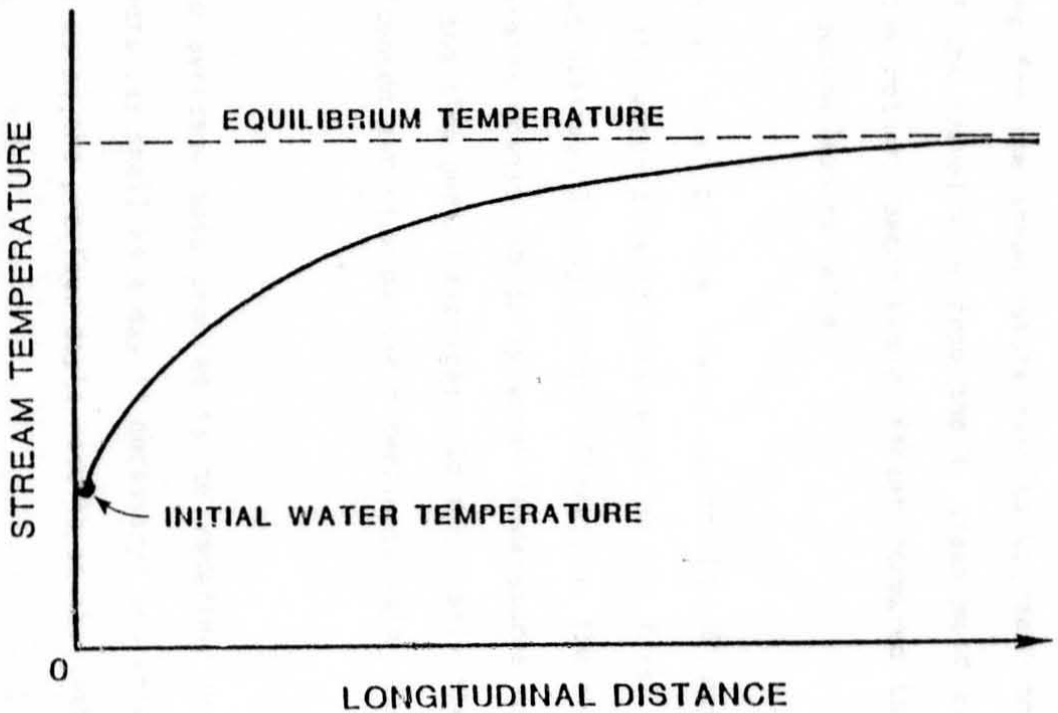

Figure 2.6. Typical longitudinal water temperature profile predicted by heat transport equation.

TIME PERIODS

The basic math model for the overall basin network is a steady-state model because it assumes that the input is a constant over an indefinite period of time. Conceptually it assumes that the input conditions exist sufficiently long for the steady-state results to reach the lowest point in the network. If the travel time from the upstream most point to the downstream end of the network becomes significant compared to the time period, then the results become less reliable.

If the travel time to the lowest point is 30 days, it should be recognized that the water passing this point on the first day of the 30 day period originated upstream 30 days prior. Therefore, the meterological conditions that determine downstream daily water temperatures on the first day are not included in the time period averages. In fact, only the last day's water column was influenced entirely by the meterologic data used in the input for the time period.

One way to overcome this problem is to redefine the time periods to smaller increments (as small as a day if necessary) and track each day's water column movement using the previous day's results as the initial conditions for the current day.

DIURNAL FLUCTUATIONS

The following relationships can be solved explicitly at any study site or point of interest to determine the maximum temperature rise of the water above the average. It is based upon the fact that the water temperature passes through the average values twice each day. That the average water temperature occurs approximately half way through the day. That the remainder of the day the water temperature increases steadily to a maximum close to sunset. The same logic is used for determining the minimum water temperature by substituting nighttime conditions in lieu of daytime.

$$d = \{[(Q/\bar{B})n]/[\sqrt{\bar{S}_e}]\}^{3/5} \qquad (\ )$$

$$t_x = (S_o/2)\ 3600 \qquad (\ )$$

$$T_{ox} = T_{ed} - \{(T_{ed} - T_{wd}) \exp [(K_d t_x)/(\rho c_p d)]\} \qquad (\ )$$

$$T_{wx} = T_{ex} - \{(T_{ex} - T_{ox}) \exp [-(K_x t_x)/(\rho c_p d)]\} \qquad (\ )$$

where: $d \equiv$ average flow depth, m.

$n \equiv$ Manning's n-value.

$Q \equiv$ discharge, cms.

$\bar{B} \equiv$ average top width, m.

$S_e \equiv$ energy gradient, m/m.

$t_x \equiv$ travel time from noon to sunset, sec.

$S_o \equiv$ duration of possible sunshine from sunrise to sunset, hours.

$T_{ed} \equiv$ equilibrium temperature for average daily conditions, C.

$T_{ex} \equiv$ equilibrium temperature for average daytime conditions, C.

T_{wd} ≡ average daily water temperature (at solar noon) at point of interest, C.

T_{ox} ≡ average daily water temperature at travel time distance upstream from point of interest, C.

T_{wx} ≡ average maximum daytime water temperature (at sunset) at point of interest, C.

K_d ≡ first order thermal exchange coefficient for daily conditions, $J/m^2/sec/C$.

K_x ≡ first order thermal exchange coefficient for daytime conditions, $J/m^2/sec/C$.

ρ ≡ density of water = 1000 kg/m^3.

c_p ≡ specific heat of water = 4182 J/kg/C.

Because of the symmetery assumed for the daytime conditions, it is only necessary to calculate the difference between the maximum daytime and average daily water temperatures to obtain the minimum water temperature.

$$T_{wn} = T_{wd} - (T_{wx} - T_{wd}) \qquad (\ )$$

where: T_{wn} ≡ average minimum nightime water temperature (at sunrise) at point of interest, C.

T_{wx} ≡ average maximum daytime water temperature (at sunset) at point of interest, C.

T_{wd} ≡ average daily water temperature (at solar noon) at point of interest, C.

FLOW MIXING

The equation for determining the final downstream water temperature when flows of different temperatures and discharges met at junctions, etc. is:

$$T_J = (T_B Q_B + T_T Q_T)/(Q_B + Q_T) \qquad (\ )$$

where: $T_J \equiv$ water temperature below junction

$T_B \equiv$ water temperature above junction on the mainstem (branch node)

$T_T \equiv$ water temperature above junction on the tributary (terminal node of the tributary)

$Q_B \equiv$ discharge above junction on the mainstem (branch node)

$Q_T \equiv$ discharge above junction on the tributary (terminal node on the tributary)

REGRESSION MODELS

Regression modesl are commonly used to smooth data and/or fill-in missing data. They are used as a part of the instream water temperature model: first, to provide initial water temperatures at headwaters or point sources to start the transport mode; and second, as an independent prediction of water temperatures at interior network points for purposes of validation and calibration. Obviously, regression models are only useful at the points of analysis and cannot be used in lieu of longitudinal transport. Two regression models are included in the instream water temperature model package: (1) a standard regression model, and (2) a transformed regression model. Each requires measured or known water temperatures as the dependent variable along with associated meteorological, hydrological, and stream geometry independent parameters. However, the standard regression model requires less detail than the transformed. The standard model is satisfactory for most applications, but the transformed version has a better physical basis. The choice becomes a matter of judgement by the responsible engineer/scientist.

STANDARD REGRESSION MODEL

IFG studies during the model development have shown that the following simple linear multiple regression model provides a high degree of correlation for natural conditions. The model is:

$$\hat{T}_w = a_0 + a_1 T_a + a_2 W_a + a_3 R_h + a_4 (S/S_o) + a_5 H_{sx} + a_6 Q$$

where: $\hat{T}_w$ ≡ estimate of water temperature, C

a_0-a_6 ≡ regression coefficients

T_a ≡ air temperature, C

W_a ≡ wind speed, mps

R_h ≡ relative humidity, decimal

S/S_o ≡ sunshine ratio, decimal

H_{sx} ≡ extra terrestrial solar radiation, $J/m^2/sec$

Q ≡ discharge, cms

It is recommended that the meterological parameters and the solar radiation at the meterological station be used for each regression analysis. Obviously, the discharge, Q, and the dependent variable water temperatures must be obtained at the point of analysis.

These six independant variables are readily obtainable and are also necessary for the transport model. A minimum of seven data sets are necessary to obtain a solution. However, a greater number is desirable for statistical validity. Also, it needs to be emphasized that the resulting regression model is only valid at the point of analysis and only if upstream hydrologic conditions do not change. For example, if a reservoir has been constructed upstream subsequent to the data set, the model is not likely to be valid because the release temperatures have been affected.

TRANSFORMED REGRESSION MODEL

The best regression model would be one that not only uses the same parameters as the best physical-process models; but has the same, or nearly the same, mathematical form. That is, the regression model equation uses physical-process transformed parameters as the independent variables. This transformed regression model uses all of the input parameters used in the transport model except for stream distance and initial water temperatures.

The first-order approximation of the constant-discharge heat transport model was chosen as the basis for the physical-process regression model. Water temperature and discharge data at the specified location together with the corresponding time period meterologic data from a nearby station are needed. The meteorologic data is used to determine the equilibrium temperature (T_e) and first-order thermal exchange coefficient (K_1). The T_e and K_1 are combined with the corresponding time period discharges as independent variables to determine the regression coefficients for estimating the corresponding time period water temperature dependent variable. An estimate of the average stream width W above the site location is necessary as an arbitrary constant in the regression. The resulting regression coefficients are tantamount to synthetically determining an upstream source water temperature as a function of time and the distance to the source.

The constant discharge heat transport model is:

$$T_w = T_o + (T_e - T_o)\,\{1-\exp[-(K_1\bar{B}x_o)/(\rho c_p Q)]\} \qquad (\ )$$

where: $T_e \equiv$ equilibrium water temperature, C

$T_o \equiv$ initial water temperature, C

$T_w \equiv$ water temperature at x_o, C

$K_1 \equiv$ first-order thermal exchange coefficient, J/m²/sec/C

$\bar{B} \equiv$ average stream width, m

$x_o \equiv$ distance from T_o, m

$\rho \equiv$ water density = 1000 kg/m³

$c_p \equiv$ specific heat of water = 4182 J/kg

$Q \equiv$ discharge, cms

The definition of $\exp(x) = e^x$ is

$$e^x = 1 + x + x^2/2! + x^3/3! + \cdots \qquad (\ )$$

If T_o is a function of the time period only, then it can be approximated as

$$T_o = \bar{T}_o + \Delta T_o \cos[(2\pi/365)\ (D_i - 213)] \qquad (\ )$$

where: $\bar{T}_o \equiv$ average initial water temperature over all time periods; C

$\Delta T_o \equiv$ half initial temperature range over all time periods; C

$D_i \equiv$ average Julian day for i^{th} time period; January 1 = 1 and December 31 = 365.

Let, $$Z_1 = -(K_1\bar{B})/(\rho c_p Q) \qquad (\ )$$

$$Z_2 = -\bar{T}_e \qquad (\ )$$

$$Z_3 = \cos[(2\pi/365)\ (D_i - 213)] \qquad (\ )$$

If equations C2 through C5 are substituted into equation C1 and the terms rearranged, then T_w can be expressed as:

$$T_w = \bar{T}_o + (\Delta T_o)Z_3 + (\bar{T}_o x_o)Z_1 + (\Delta T_o x_o)Z_1 Z_3$$
$$+ (x_o)Z_1 Z_2 + (\bar{T}_o x_o^2/2)Z_1^2 + (\Delta T_o x^2/2)Z_1^2 Z_3$$
$$+ (x_o^2/2)Z_1^2 Z_2 + (\bar{T}_o x_o^3/6)Z_1^3 + (\Delta T_o x_o^3/6)Z_1^3 Z_3$$
$$+ (x_o^3/6)Z_1^3 Z_2 + (\bar{T}_o x_o^4/24)Z_1^4 + (\Delta T_o x_o^4/24)Z_1^4 Z_3$$
$$+ (x_o^4/24)Z_1^4 Z_2 + \cdots \qquad (\ )$$

If the converging power series is truncated after the final fourth-order term and the following substitutions are made, then a possible multiple linear regression model results.

Let,

$a_o = \bar{T}_o$	
$a_1 = \Delta T_o$	$X_1 = Z_3$
$a_2 = \bar{T}_o x_o$	$X_2 = Z_1$
$a_3 = \Delta T_o x_o$	$X_3 = Z_1 Z_3$
$a_4 = x_o$	$X_4 = Z_1 Z_2$
$a_5 = \bar{T}_o x_o^2/2$	$X_5 = Z_1^2$
$a_6 = \Delta T_o x_o^2/2$	$X_6 = Z_1^2 Z_3$
$a_7 = x_o^2/2$	$X_7 = Z_1^2 Z_2$
$a_8 = \bar{T}_o x_o^3/2$	$X_8 = Z_1^3$
$a_9 = \Delta T_o x_o^3/6$	$X_9 = Z_1^3 Z_3$
$a_{10} = x_o^3/6$	$X_{10} = Z_1^3 Z_2$
$a_{11} = \bar{T}_o x_o^4/2$	$X_{11} = Z_1^4$

$$a_{12} = \Delta T_0 x_0^4/24 \qquad X_{12} = Z_1^4 Z_3$$

$$a_{13} = x_0^4/24 \qquad X_{13} = Z_1^4 Z_2$$

If the resulting independent transformed variables X_1, through X_{13} are regressed on the dependent variable T_w, then the following regression equation results

$$\hat{T}_w = a_0 + a_1 X_1 + \cdots + a_{13} X_{13} \qquad (\ )$$

The best estimates of the synethic physical-process parameters are

$$\bar{T}_0 = a_0 \qquad (\ )$$

$$\Delta T_0 = a_1 \qquad (\ )$$

$$x_0 = a_4 \qquad (\ )$$

Attachment 2

HEAT FLUX COMPONENTS FOR AVERAGE
MAINSTEM SUSITNA CONDITIONS

Sources of heat flux calculation by USGS

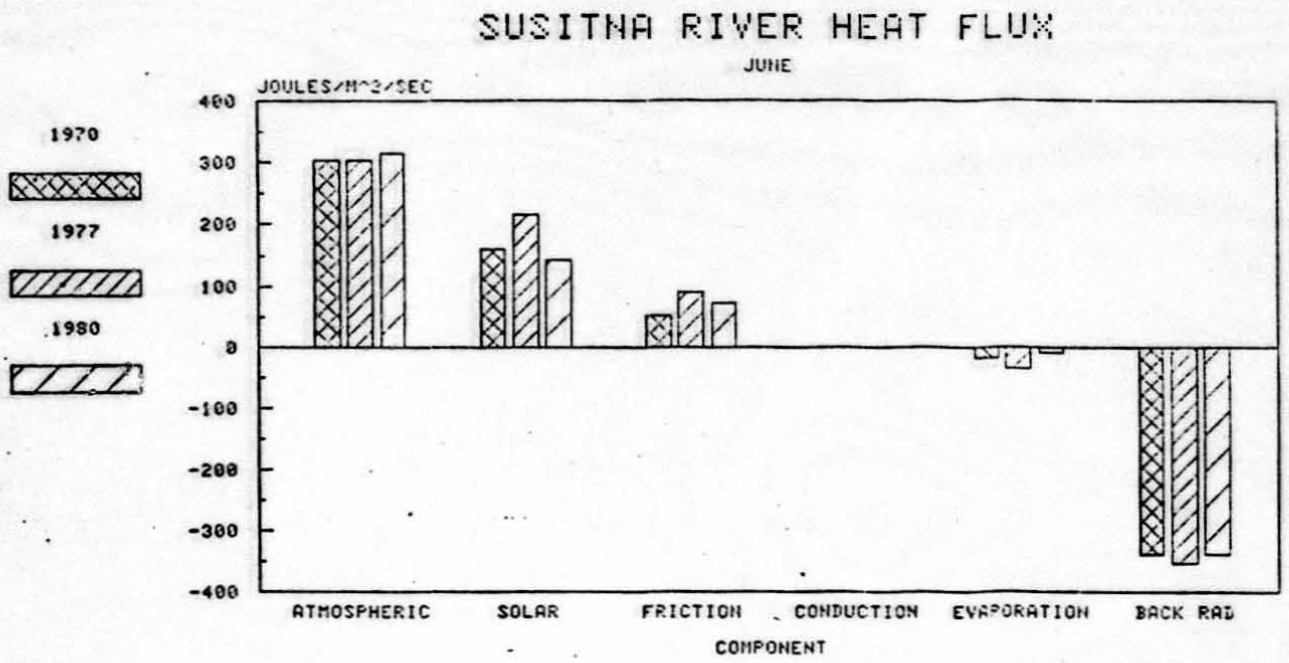

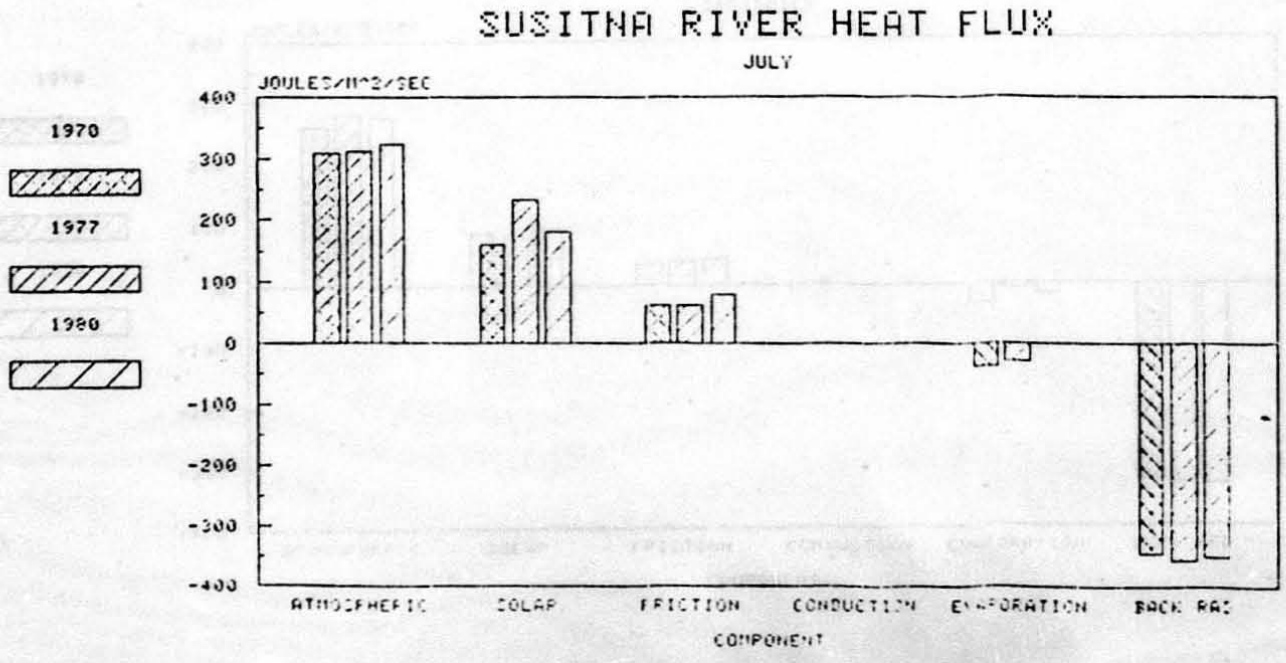

Sources of heat flux calculated by SNTEMP.

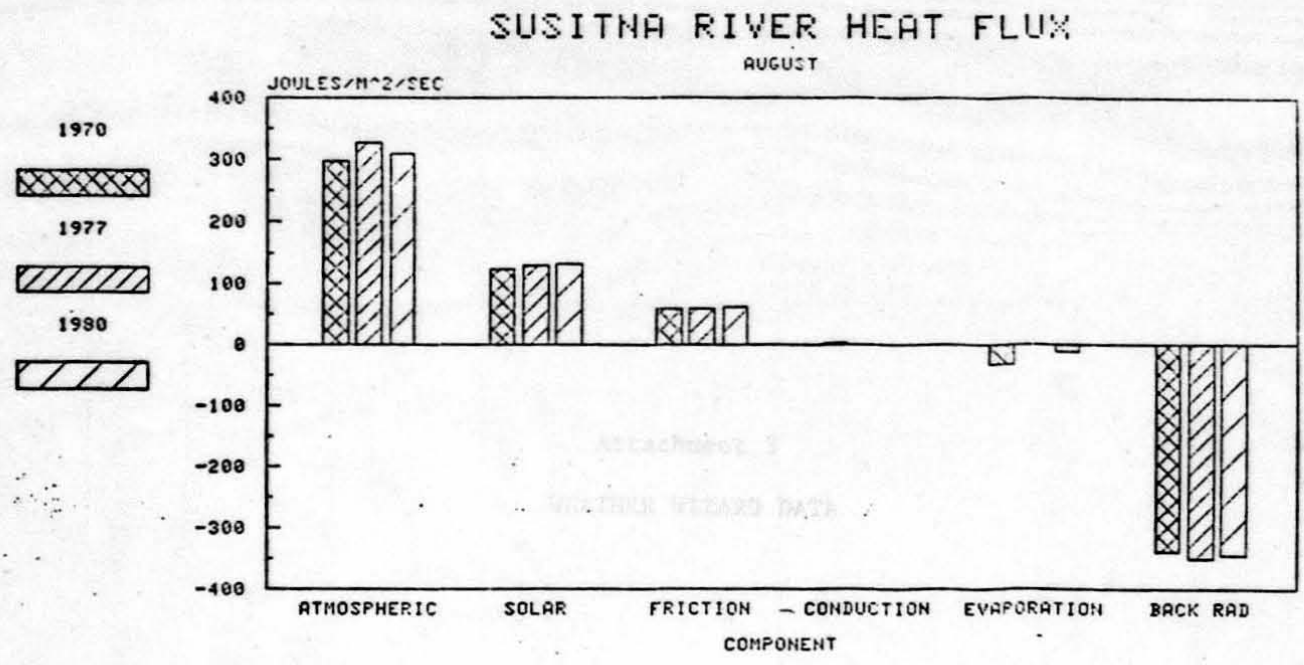

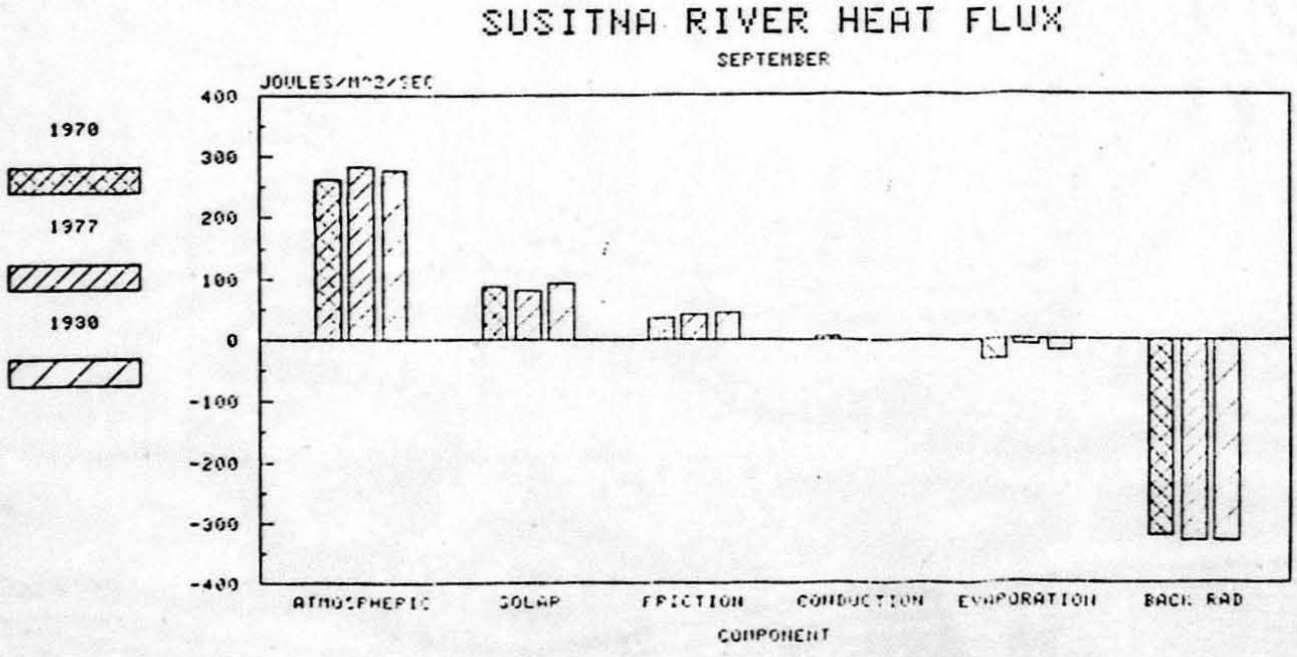

Attachment 3

WEATHER WIZARD DATA

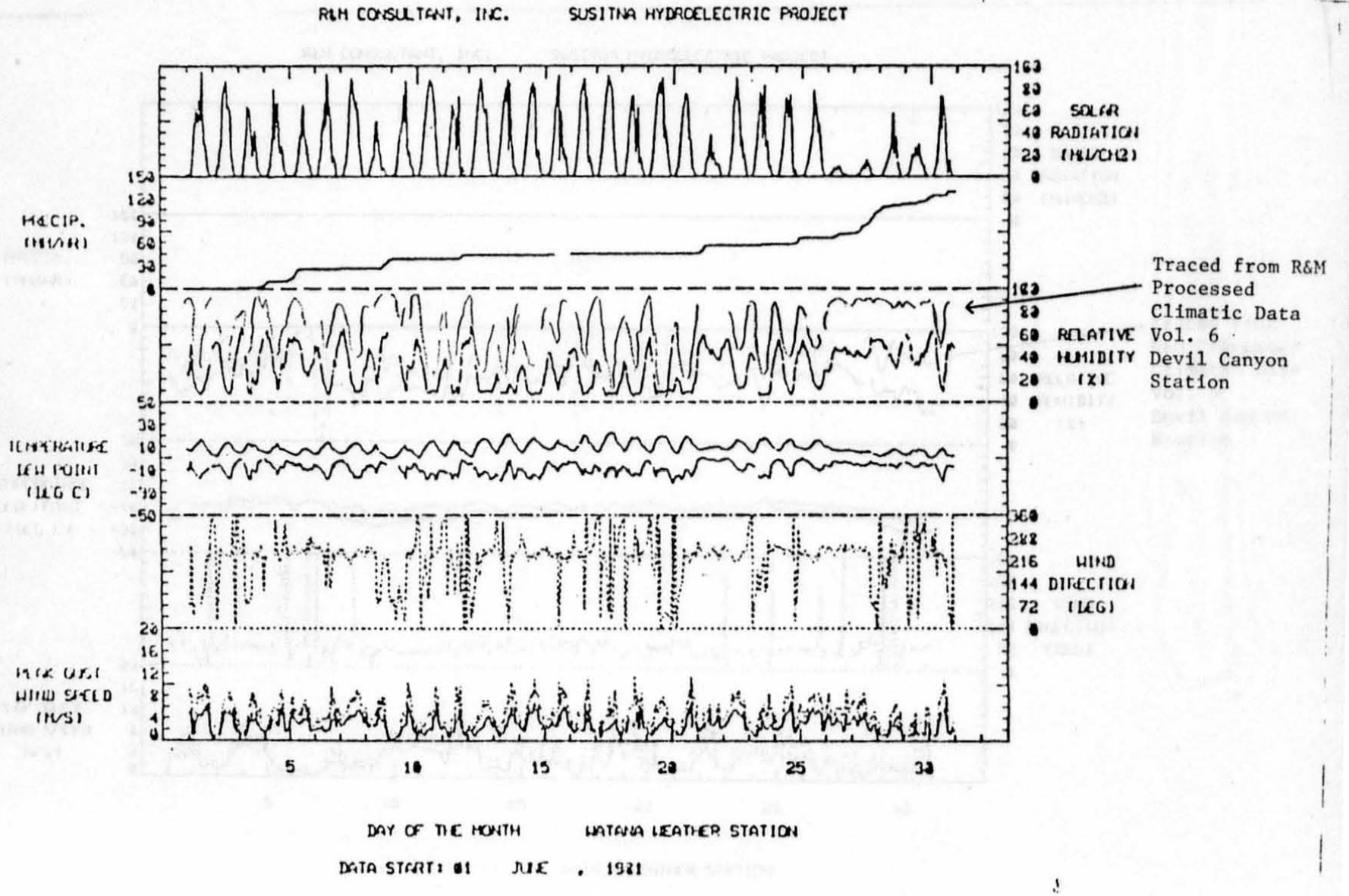

Traced from R&M Processed Climatic Data Vol. 6 Devil Canyon Station

From R&M Processed Climatic Data, Vol. 5, Watana Station

Figure 1

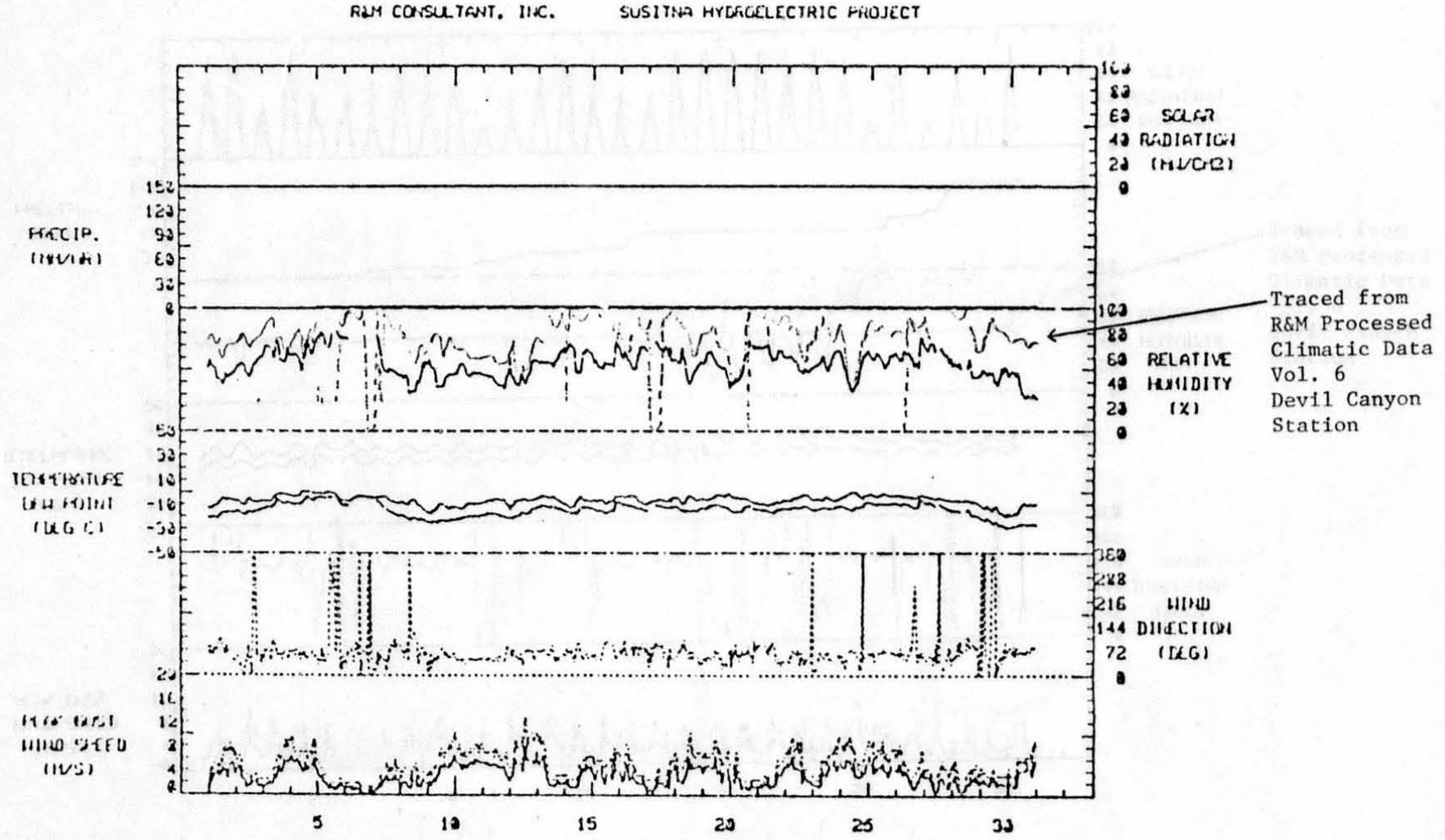

Traced from R&M Processed Climatic Data Vol. 6 Devil Canyon Station

From R&M Processed Climatic Data, Vol. 5, Watana Station

Figure 2

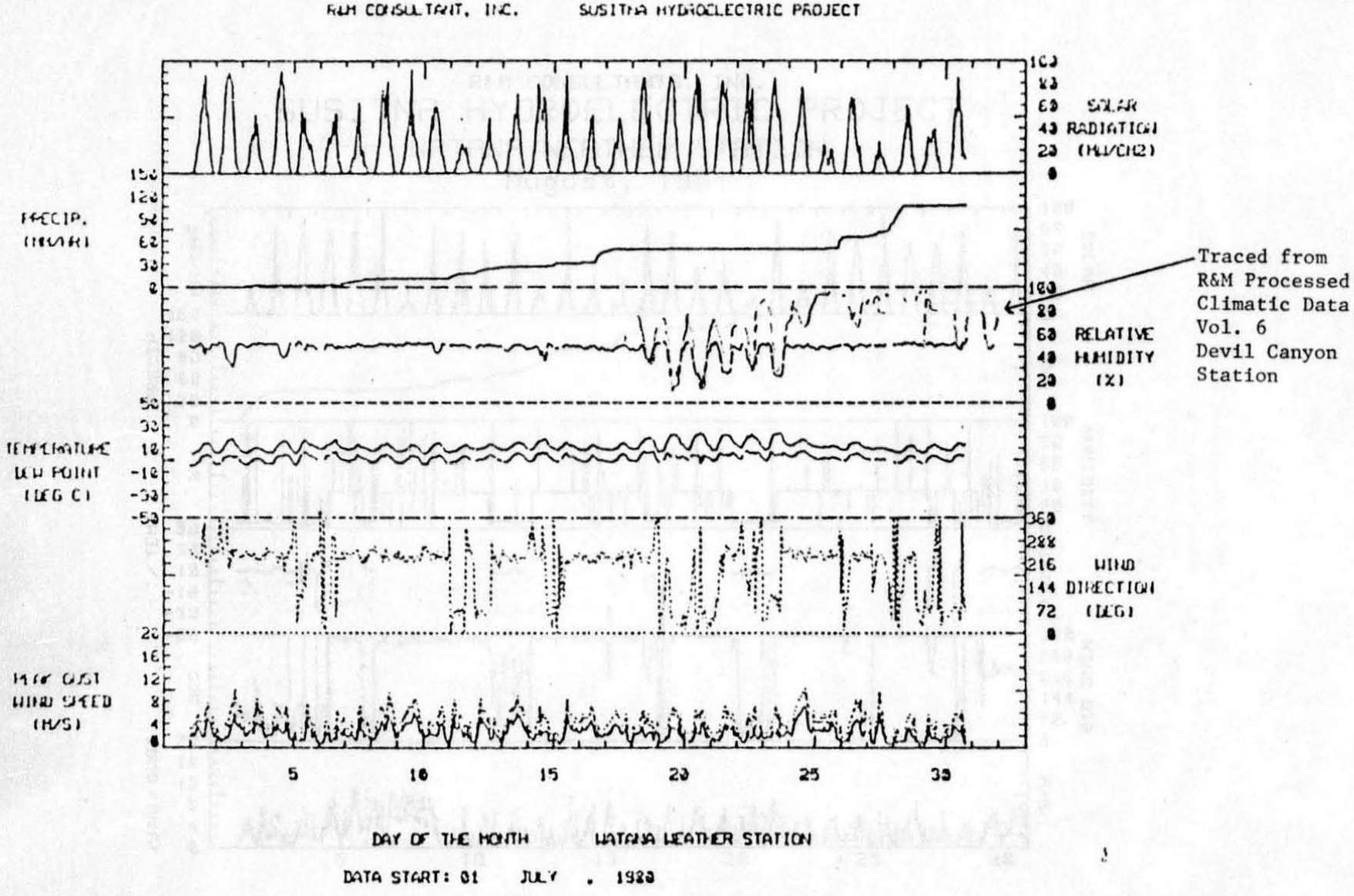

Traced from R&M Processed Climatic Data Vol. 6 Devil Canyon Station

From R&M Processed Climatic Data, Vol. 5, Watana Station

Figure 3

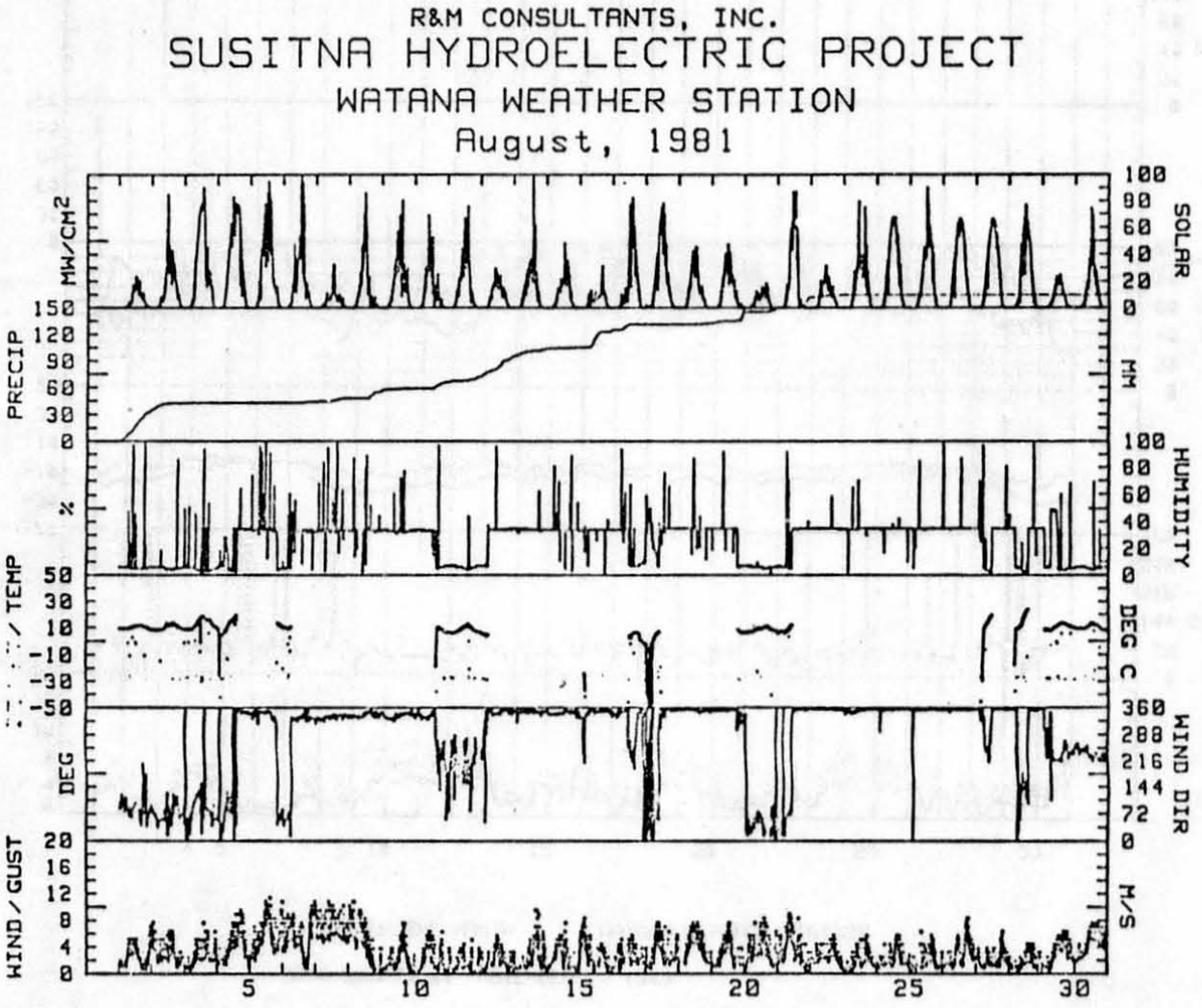

From R&M Processed Climatic Data, Vol. 5, Watana Station

Figure 4

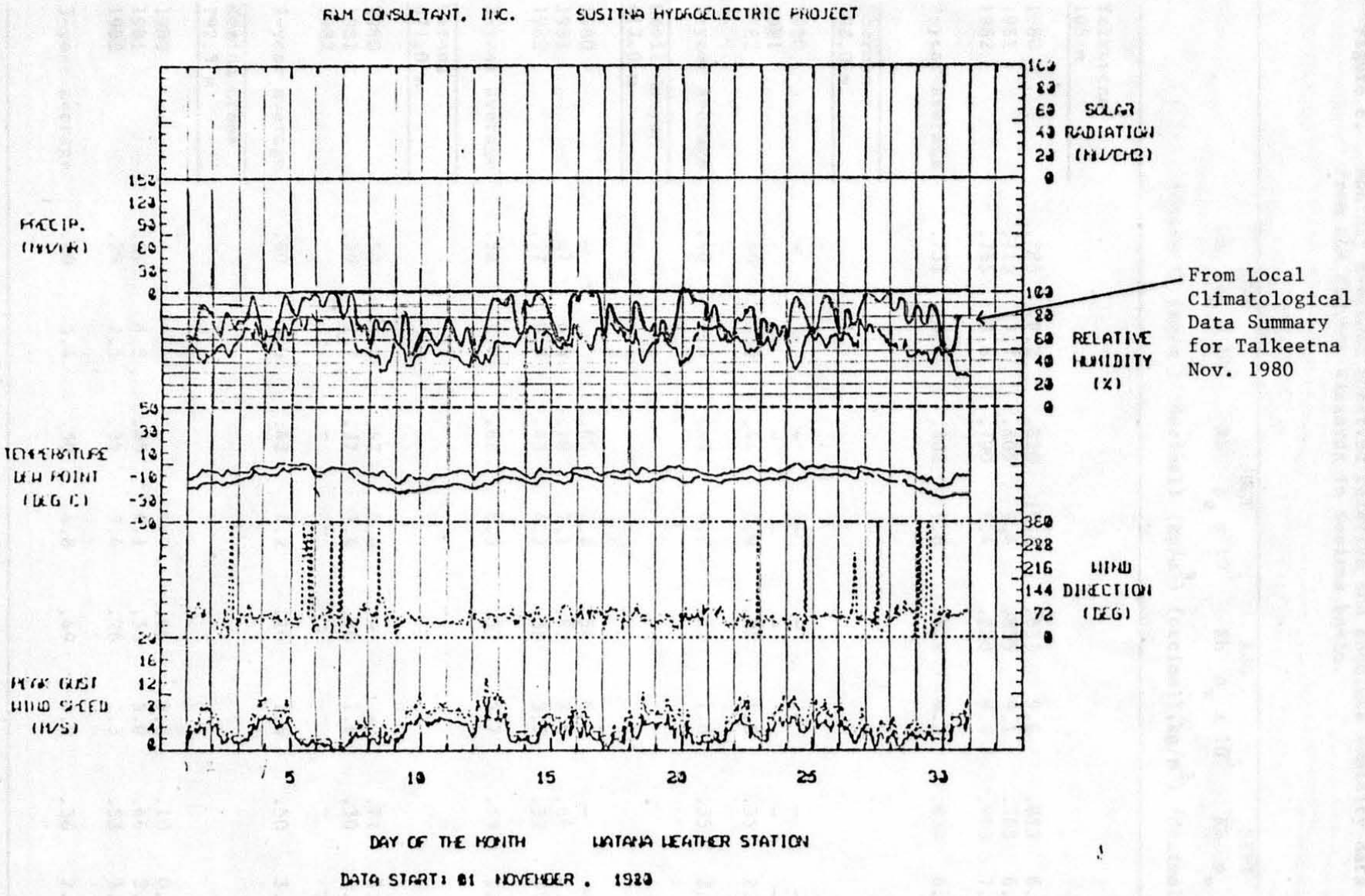

From R&M Processed Climatic Data, Vol. 5, Watana Station

Figure 5

Figure 6. Monthly averaged observed relative and absolute humidity data from R&M Weather Wizzards in Susitna basin.

	JUNE		JULY		AUG		SEPT	
	Rh (decimal)	$\rho_v \times 10^5$ (kg/m^3)	Rh (decimal)	$\rho_v \times 10^5$ (kg/m^3)	Rh (decimal)	$\rho_v \times 10^5$ (kg/m^3)	Rh (decimal)	$\rho_v \times 10^5$ (kg/m^3)
Talkeetna[1] 105 m								
1980	.785	8.2	.810	10.0	.833	9.0	.813	6.7
1981	.713	7.7	.805	9.4	.835	9.1	.785	6.7
1982	.755	8.6	.790	9.4	.820	9.4	.903	7.0
3-year average	.751	8.2	.802	9.6	.829	9.2	.834	6.8
Sherman 198.0 m								
1980	-	-	-	-	-	-	-	-
1981	-	-	-	-	-	-	-	-
1982	.40	4.0	.44	4.9	.22	1.8	.35	2.8
3-year average	.40	4.0	.44	4.9	.22	1.8	.35	2.8
Devil Canyon 457.0 m								
1980	-	-	.65	7.6	.54	6.0	-	-
1981	.67	6.4	.78	7.1	.82	7.6	.66	4.2
1982	.37	3.5	.43	4.2	.35	3.5	.52	3.9
3-year average	.52	5.0	.62	6.3	.57	5.7	.59	2.7
Watana 671.0 m								
1980	.50	4.5	.47	5.0	-	-	.71	5.0
1981	.29	2.7	.37	3.4	.26	1.6	.30	2.0
1982	-	-	-	-	-	-	-	-
3-year average	.40	3.6	.42	4.2	.26	1.6	.50	3.5
Kosina Creek 792.5 m								
1980	-	-	-	-	.66	5.2	.10	0.6
1981	.51	4.3	.65	6.1	.56	5.0	.46	2.7
1982	.29	2.5	.35	3.4	.26	2.3	.53	3.6
3-year average	.40	3.4	.50	4.8	.49	4.2	.36	2.3

[1]Data from National Weather Service Local Climatological Data Summary

Figure 7. Monthly averaged observed temperature (°C) from R&M Weather Wizzard.

	JUNE	JULY	AUG	SEPT
Talkeetna[1] 105.0 m				
1980	11.9	14.7	12.1	7.7
1981	12.2	13.5	12.4	7.7
1982	11.7	13.7	13.2	7.8
3-year average	11.9	14.0	12.6	7.7
Sherman 198.0 m				
1980	-	-	-	-
1981	-	-	-	-
1982	10.7	12.8	11.6	7.1
3-year average	10.7	12.8	11.6	7.1
Devil Canyon 457.0 m				
1980	-	13.7	12.5	-
1981	10.0	9.3	9.2	3.3
1982	9.9	11.7	10.8	6.0
3-year average	10.0	11.6	10.8	4.7
Watana 671.0 m				
1980	9.1	11.9	-	4.8
1981	9.3	9.3	2.0	4.0
1982	8.6	10.8	10.0	5.0
3-year average	9.0	10.7	6.0	4.6
Kosina Creek 792.5 m				
1980	-	-	6.8	3.1
1981	8.0	9.7	9.0	2.9
1982	8.4	10.4	9.1	4.4
3-year average	8.2	10.1	8.3	3.5

[1] Data from National Weather Service Local Climatological Data Summary

Attachment 4

DAILY INDIAN RIVER TEMPERATURES VERSUS
DEVIL CANYON AIR TEMPERATURES

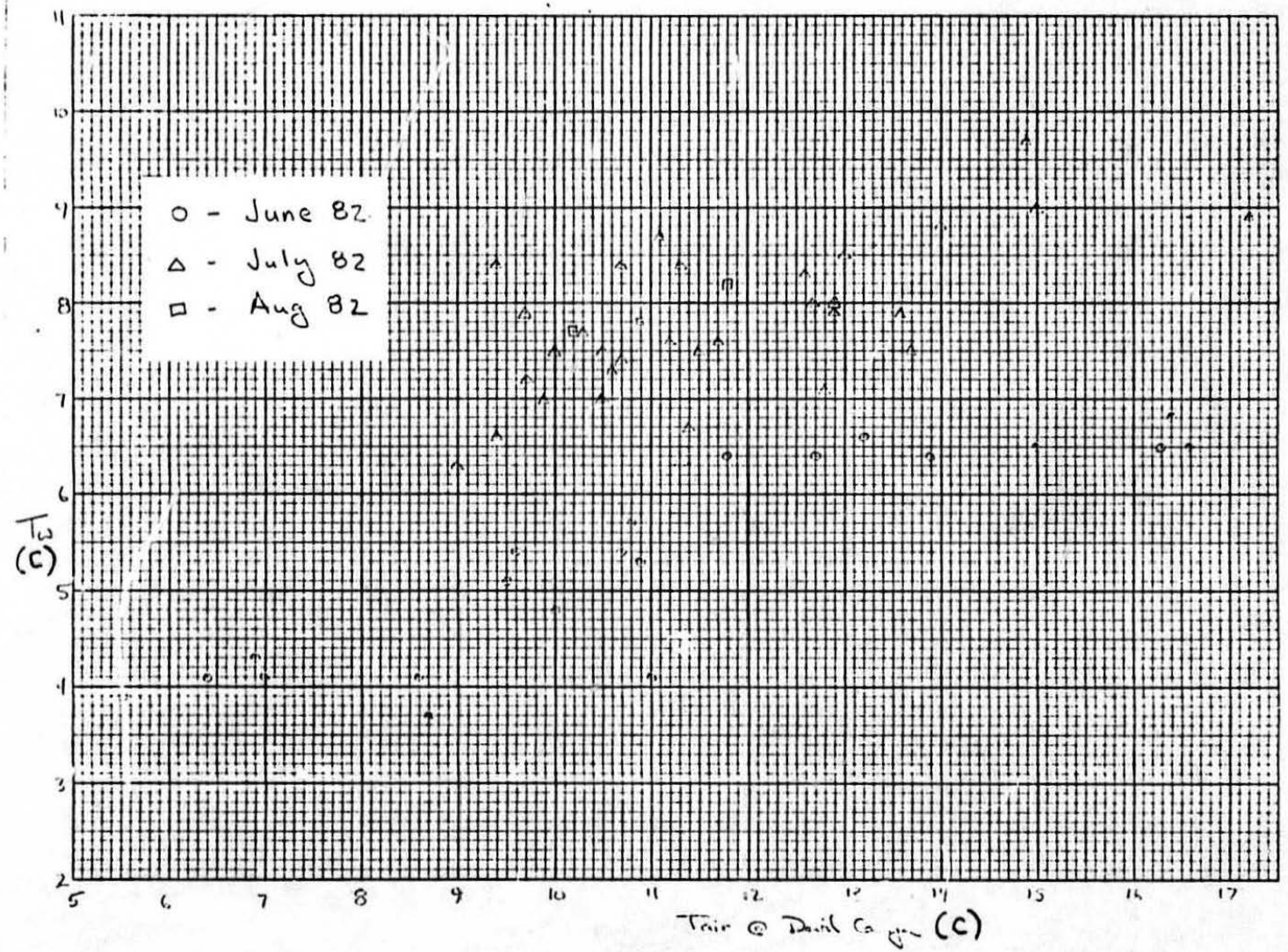
o - June 82
Δ - July 82
□ - Aug 82
T_w (C)
Tair @ Dark Gauge (C)